



The *Aspergillus fumigatus* Sialidase (Kdnase) Contributes to Cell Wall Integrity and Virulence in Amphotericin B-Treated Mice

Jason R. Nesbitt^{1†}, Elizabeth Y. Steves^{1†}, Cole R. Schonhofer¹, Alissa Cait², Sukhbir S. Manku³, Juliana H. F. Yeung¹, Andrew J. Bennet⁴, Kelly M. McNagny², Jonathan C. Choy³, Michael R. Hughes² and Margo M. Moore^{1*}

¹ Department of Biological Sciences and the Centre for Cell Biology, Development and Disease, Simon Fraser University, Burnaby, BC, Canada, ² Biomedical Research Centre, The University of British Columbia, Vancouver, BC, Canada, ³ Department of Molecular Biology and Biochemistry, Simon Fraser University, Burnaby, BC, Canada, ⁴ Department of Chemistry, Simon Fraser University, Burnaby, BC, Canada

OPEN ACCESS

Edited by:

Frederic Lamoth,
Centre Hospitalier Universitaire
Vaudois (CHUV), Switzerland

Reviewed by:

Praveen Rao Juvvadi,
Duke University, United States
Jarrod R. Fortwendel,
University of South Alabama,
United States
Iran Malavazi,
Federal University of São Carlos,
Brazil

*Correspondence:

Margo M. Moore
mmoore@sfu.ca

[†] These authors have contributed
equally to this work.

Specialty section:

This article was submitted to
Fungi and Their Interactions,
a section of the journal
Frontiers in Microbiology

Received: 02 November 2017

Accepted: 29 December 2017

Published: 18 January 2018

Citation:

Nesbitt JR, Steves EY,
Schonhofer CR, Cait A, Manku SS,
Yeung JHF, Bennet AJ,
McNagny KM, Choy JC, Hughes MR
and Moore MM (2018) The
Aspergillus fumigatus Sialidase
(Kdnase) Contributes to Cell Wall
Integrity and Virulence
in Amphotericin B-Treated Mice.
Front. Microbiol. 8:2706.
doi: 10.3389/fmicb.2017.02706

Aspergillus fumigatus is a filamentous fungus that can cause a life-threatening invasive pulmonary aspergillosis (IPA) in immunocompromised individuals. We previously characterized an *exo*-sialidase from *A. fumigatus* that prefers the sialic acid substrate, 2-keto-3-deoxy-D-glycero-D-galacto-nononic acid (Kdn); hence it is a Kdnase. Sialidases are known virulence factors in other pathogens; therefore, the goal of our study was to evaluate the importance of Kdnase in *A. fumigatus*. A *kdnase* knockout strain ($\Delta kdnase$) was unable to grow on medium containing Kdn and displayed reduced growth and abnormal morphology. $\Delta kdnase$ was more sensitive than wild type to hyperosmotic conditions and the antifungal agent, amphotericin B. In contrast, $\Delta kdnase$ had increased resistance to nikkomycin, Congo Red and Calcofluor White indicating activation of compensatory cell wall chitin deposition. Increased cell wall thickness and chitin content in $\Delta kdnase$ were confirmed by electron and immunofluorescence microscopy. In a neutropenic mouse model of invasive aspergillosis, the $\Delta kdnase$ strain had attenuated virulence and a significantly lower lung fungal burden but only in animals that received liposomal amphotericin B after spore exposure. Macrophage numbers were almost twofold higher in lung sections from mice that received the $\Delta kdnase$ strain, possibly related to higher survival of macrophages that internalized the $\Delta kdnase$ conidia. Thus, *A. fumigatus* Kdnase is important for fungal cell wall integrity and virulence, and because Kdnase is not present in the host, it may represent a potential target for the development of novel antifungal agents.

Keywords: invasive aspergillosis, sialidase, cell wall integrity, chitin, Kdn

INTRODUCTION

Aspergillus fumigatus is a filamentous fungus that can cause a life-threatening systemic mycosis called invasive aspergillosis (IA). IA cases are rare in immunocompetent patients but affect those with weakened immune systems caused by immunosuppressive drug treatment, cancer or genetic polymorphisms that affect the innate immune response (Schmiedel and Zimmerli, 2016).

IA typically begins in the lungs after inhalation of airborne fungal conidiospores (conidia) that attach to the epithelium and germinate. If the epithelial barrier is breached, the fungus may disseminate hematogenously to other organs such as the brain or kidneys (Young et al., 1970). Other less common portals of entry for invasive *Aspergillus* infection include the skin, gastrointestinal tract, and the eyes (Fuqua et al., 2010). IA is usually treated with the triazole antifungal, voriconazole as the primary treatment, and the polyene antibiotic, amphotericin B as an alternative. Caspofungin, an echinocandin antifungal agent, is utilized as a salvage therapy as it is generally less toxic than the other two drugs (Walsh et al., 2008; Kousha et al., 2011). Despite drug treatment, the overall mortality rate for IA is approximately 50% and other factors can worsen prognosis, such as the progression of underlying malignancy, renal impairment, or recent corticosteroid treatment (Nivoix et al., 2008).

There are more than 250 species in the *Aspergillus* genus. Most invasive infections are caused by members of the *A. fumigatus* species complex followed by organisms in the *A. terreus*, *A. flavus*, and *A. niger* complexes (Lass-Flörl and Cuenca-Estrella, 2017). Fungal pathogenesis is complex and requires the normally saprotrophic *Aspergillus* spp. to adapt to the environment of the human lung. Numerous excellent reviews have summarized the pathways or molecules that contribute to the ability of *A. fumigatus* to colonize and invade host tissue including transcription factors (Bultman et al., 2017), secondary metabolites such as toxins or siderophores (Scharf et al., 2014) and immune evasion factors (Chotirmall et al., 2014). Binding to host tissues is an important first step in establishing an infection. *A. fumigatus* secretes the polysaccharide, galactosaminogalactan (GAG) that has been implicated in both adhesion to host tissue (biofilm formation) and virulence (Gravelat et al., 2013). GAG also contributes to immunosuppression by inducing apoptosis of neutrophils (Robinet et al., 2014).

Adhesion of *A. fumigatus* conidia to the host is also mediated by sialic acids. Sialic acids are a family of >50 derivatives of the 9-carbon monosaccharide, neuraminic acid. Two naturally occurring sialic acids have a substitution at carbon 5 with an *N*-acetyl or an -OH group yielding *N*-acetylneuraminic acid (Neu5Ac) or 2-keto-3-deoxy-D-glycero-D-galacto-nononic acid (Kdn), respectively (Varki and Schauer, 2009). We demonstrated previously that fungal sialic acids were responsible, in part, for binding of *A. fumigatus* conidia to fibronectin and intact basal lamina and that *A. fumigatus* contained higher levels of sialic acid on the conidial surface compared to non-pathogenic species (Wasylnka and Moore, 2000; Wasylnka et al., 2001). Enzymatic removal of sialic acids on conidia led to a decrease in their uptake by both cultured murine macrophages and cultured type 2 pneumocytes (Warwas et al., 2007). Sialic acids have also been detected on numerous other species of pathogenic fungi including *Fonsecaea pedrosoi*, *Sporothrix schenckii*, *Paracoccidioides brasiliensis*, *Cryptococcus neoformans*, and *Candida albicans* (Alviano et al., 1999).

The sialic acid biosynthetic pathway has not been identified in any fungus to date; however, we have previously identified and characterized a sialidase from *A. fumigatus*. Sialidases are glycoside hydrolase enzymes that catalyze the release

of sialic acids from glycans present on the cell surface or in their environment. The *A. fumigatus* sialidase has an N-terminal secretion sequence and may therefore have a role in modifying cell wall carbohydrates and/or cleaving extracellular carbohydrates. Recombinant *Afsialidase* cleaved terminal synthetic substrates with α 2,3-linked sialic acids to a greater extent than those with α 2,6-linked sialic acids; hydrolysis of 2,8-linked sialic acids by the *A. fumigatus* sialidase was also demonstrated (Warwas et al., 2010). Growth in medium containing human serum induced sialidase gene expression (Warwas et al., 2010). Subsequent studies revealed that the *A. fumigatus* sialidase activity was not inhibited by the classical sialidase inhibitor, 2-deoxy-2,3-didehydro-N-acetylneuraminic acid (DANA) (Telford et al., 2011). Furthermore, the crystallized *A. fumigatus* sialidase covalently bound 3-F- β -Kdn in the enzyme active site. Kinetic analysis showed that the catalytic efficiency (k_{cat}/K_m) was 5 orders of magnitude higher with Kdn-methylumbelliferone compared to the Neu5Ac substrate (Telford et al., 2011). Hence, the *A. fumigatus* sialidase is a Kdnase but its importance to survival of *A. fumigatus* *in vitro* and *in vivo* is unknown.

Sialidases are involved in the virulence of several mammalian pathogens. For example, viral sialidase is critical for completing the life cycle of influenza virus as it prevents viral recapture upon budding (Palese et al., 1974). Sialidase activity is also important for the virulence of several bacterial pathogens. For example, *S. pneumoniae* expresses three sialidases: NanA, NanB, and NanC, and a Δ nanA mutant of the R6 cell line displayed reduced adherence to D562 human pharyngeal cells and a decrease in biofilm formation (King et al., 2006). Recent evidence has revealed that internalization of *Salmonella* ser. Typhimurium is dependent on glycoside hydrolases including the sialidase, NanH. Deletion of *nanH* resulted in a decrease of adhesion and invasion of Caco-2 cells equivalent to the level observed with mutants of the Type III secretion system (T3SS) (Arabyan et al., 2016).

The goals of the present study were to determine whether the *Aspergillus fumigatus* sialidase (Kdnase) is critical for the growth and development of *A. fumigatus* and whether it is required for virulence. Specifically, we examined the phenotypes and cell wall carbohydrates of the parental, Kdnase mutant; and, complemented strains grown in various carbon sources and under conditions of cell wall stress, including the effect of antifungal agents. The interaction of conidia with macrophages *in vitro* was also investigated. Finally, we determined the relative virulence of the strains in a neutropenic mouse model of IA.

MATERIALS AND METHODS

A. fumigatus Strains and Growth Conditions

Aspergillus fumigatus strain ATCC 13073 (American Type Culture Collection, Manassas, VA, United States), originally isolated from a human pulmonary lesion, was used throughout this study as the wild type (WT) or parental strain. Unless stated otherwise, fungi were grown at 37°C on yeast extract-agar-glucose (YAG, 0.5% yeast extract, 2% glucose, 0.125%

MgSO₄•7H₂O, 0.1% Hutner's trace elements, 0.1% Vitamins, 1.5% agar) or Kafer's minimal medium (Hill and Kafer, 2001) supplemented with Hutner's trace elements and vitamins. All strains were stored on silica gel at -80°C.

Harvesting Conidia

Mature conidia were harvested by flooding an agar plate with phosphate-buffered saline, pH 7.4 supplemented with 0.05% Tween 20 (PBST). The surface was gently agitated with a sterile cotton swab and the suspension was filtered through sterile Mira cloth (Calbiochem) to remove hyphal fragments. Conidia were then washed three times in sterile PBS. Spores were counted with a haemocytometer.

Fungal Growth on Varying Carbon Sources or Stressors

Kafer's minimal media with a 1% Hutner's vitamin mixture was used to compare the growth of wild type and $\Delta kdnase$ *A. fumigatus* strains. The carbon source was changed as indicated. Equivalent numbers of conidia were inoculated into the center of each plate and plates were incubated for 72 h at 37°C. Hygromycin (100 µg/mL) was the positive selection marker. To test the effect of sorbitol on growth, YAG solid media plates (with or without 1 M sorbitol) were inoculated with 10⁵ conidia, in a volume of 5 µL in the center of each plate. Slide cultures were also prepared for each strain on YAG supplemented with 750 µg/mL Congo Red dye and incubated for 20 h at 37°C. Images were obtained on a Zeiss inverted microscope at 100× magnification.

A. fumigatus Growth Assays in the Presence of Antifungal Drugs

Growth assays were prepared and monitored following the EUCAST protocol (EUCAST E.DEF 9.3 December 2015) modified by addition of resazurin to increase the sensitivity of growth measurement (Yamaguchi et al., 2002). Assays were prepared in 96-well microdilution plates with RPMI 1640 media buffered with 3-(*N*-morpholino)propanesulfonic acid (MOPS) at a final concentration of 0.165 M, pH 7.0, and 2 × 10⁵ conidia/mL. Antifungal compounds were prepared in dimethyl sulfoxide (DMSO) to a maximum of 2.5% v/v. Control wells contained DMSO alone. Resazurin stock solution (Sigma-Aldrich) was prepared in PBS and filter sterilized, and media were prepared with a final concentration of 0.02% resazurin. Plates were incubated in the dark at 37°C. Growth was quantified in a SpectraMax plate reader by measuring resorufin fluorescence after 36–48 h of incubation (excitation wavelength 560 nm; emission wavelength 590 nm). Control plates were done in parallel that contained all components except conidia confirmed that antibiotics did not affect resorufin fluorescence.

Construction and Confirmation of *kdnase* Knockout Strain and Complemented Strain

The *kdnase* knockout was created by homologous recombination using a disruption construct containing 1000 bp sequences of DNA encoding the upstream and downstream regions of the

kdnase gene, flanking a positive selectable marker for hygromycin resistance (Supplementary Figure S1). The disruption construct was generated using fusion PCR and introduced into the wild type strain using *Agrobacterium*-mediated transformation as follows. The hygromycin resistance gene cassette containing the *Escherichia coli* (hygromycin phosphotransferase, *hph*) under the control of the constitutive *trpC* promoter and terminator from *Aspergillus nidulans* (Hamert and Timberlaket, 1987) was amplified with the primers 5'-AAACATTCCTACTATCGCGA TCGTGCAGCTTAACTGATATTGA and 5'-TAATGCTAGTCC AGCAACGACGTCGAC GTTAACTGGTTCC. The upstream and downstream 1000 base pairs of DNA that flank the *kdnase* gene in were amplified by PCR with the following primer pairs, upstream: 5'-GCGCTCTATCCAGTCAGTC; 5'-TCGCGATAGTGGGAATGTTT and downstream: 5'-TCG TTGCTGGACAGCATTAT; 5'-TGCTTCATGTCATGCCTAGC. The *hph* cassette and *kdnase* flanking regions were amplified by PCR using iProofTM High-fidelity DNA polymerase (Bio-Rad, Mississauga, ON, Canada). Fusion PCR was performed with high-fidelity AccuPrime *Taq* DNA polymerase (Thermo Fisher Scientific, Mississauga, ON, Canada) using the primers 5'-GGGATCCACATACCATTCTCGCCGAAC and 5'-GGGATCCAATGCTA CGGGAACACTTGG that added a *Bam*HI restriction site to facilitate insertion into the pCambia plasmid. The fusion PCR fragment was gel purified and cloned into pCambia 0380 plasmid (Cambia) yielding pCambia-KdnaseKO. Competent *Agrobacterium tumefaciens* (AGL-1) were transformed using heat shock. Transformation of *A. fumigatus* followed the protocol of Sánchez and Aguirre (1996) with modifications. Putative fungal transformants were harvested using a punch transfer tool and placed on fresh YAG agar plates containing 100 µg/mL hygromycin. Plates were incubated at 37°C for 72 h before mature spores were harvested. Conidial suspensions were then diluted and re-plated with an estimated 10 spores per plate to generate plates with colonies grown from single spores.

*Xho*I-digested DNA from the WT and mutant strains was analyzed by Southern blotting to ensure that only a single copy of the *kdnase* gene was integrated into the genome and that the integration was at the *kdnase* locus (Supplementary Figure S2). The knockout strain was also sequenced at the *kdnase* locus to ensure that up- and downstream sequences were not affected. Successful homologous integration of the knockout construct in the putative mutants was also confirmed by PCR (Supplementary Figure S3).

To construct $\Delta kdnase^R$, the rescued strain, iProof polymerase (Bio-Rad) was used to amplify 2470 base pairs of the wild type *kdnase* gene plus 928 bp of upstream sequence [including TATA and CAAT boxes (Warwas et al., 2010)] and 322 bp of downstream sequence.

The rescue construct was amplified with the primers 5'-T GCAAGCTTCAGA ACTGCCCTTCCCTCT-3' and 5'-GTT AAGCTTACTGTTTGGCTGCCCTCTTC-3' containing *Hind*III restriction sites to facilitate insertion into pBCPhleo (Silar, 1995). pBC-phleo-Kdnase was used to transform *E. coli* DH5 α and plasmid DNA was linearized with *Spe*I (New England Biolabs, Whitby, ON, Canada). Linearized plasmid DNA (10 µg) was

introduced into 50 μ L of swollen conidia by electroporation. Briefly, ice-cold swollen conidia were pelleted by centrifugation and washed 3 times with 4°C sterile water after which they were re-suspended in 4 mL YED media (1% yeast extract, 1% glucose, 20 mM HEPES, pH 8) and incubated for 1 h at 30°C with gentle shaking. Following incubation, conidia were centrifuged and re-suspended in 150 μ L of electroporation buffer (10 mM Tris-HCL pH7.5, 270 mM sucrose, and 1 mM lithium acetate). The conidial suspension was then divided into 50 μ L aliquots for use in transformation. The restriction enzyme *SpeI* (New England Biolabs) was used to linearize pBC-phleo-Kdnase. Linearized plasmid DNA (10 μ g) was added to 50 μ L of prepared conidia and the mixture was incubated for 15 min on ice before being transferred to an electroporation cuvette with a 2 mm gap. Conidia were exposed to an electric field pulse of 1 kV, 400 ohms, and 25 μ F. Immediately following the pulse, 1 mL of ice-cold YED media was added to the conidia and they were cooled on ice for 15 min before being allowed to recover for 2 h at 37°C with gentle shaking. Transformants were selected on YAG media containing 100 μ g/mL phleomycin. Putative transformants were subcultured onto selective media to obtain pure cultures. Ectopic integration of the rescue construct was confirmed using PCR (Supplementary Figure S3).

Semi-quantitative Analysis of Cell Wall Polysaccharides

α (1,3)-Glucan and β (1,3)-Glucan

Sterile glass cover slips were dried and added to Petri dishes containing 20 ml YAG with or without 1 M sorbitol. Conidia of the appropriate strain were added and allowed to germinate overnight at 37°C. Conidia incubated in medium containing sorbitol required an additional 6 h of growth. Coverslips were removed and washed with PBS and prepared for immunofluorescence microscopy as follows: for α (1,3)-glucan analysis, a mouse monoclonal antibody specific to α (1,3)-glucan (Sigma, M5170) was added to a PBS solution containing 0.5% BSA and 0.05% Tween 20 at a dilution of (1:10) and slides were incubated in the dark overnight at 4°C. After washing with PBS, an AlexaFluor 488-conjugated secondary antibody (Jackson ImmunoResearch, 1:50 dilution) was added and the coverslips were incubated for 1 h at room temperature. Coverslips were mounted on slides after rinsing with PBS and adding Prolong Gold anti-fade solution. Slides were allowed to dry, sealed with nail polish and stored at 4°C in the dark. Fluorescence was visualized on a spinning disk confocal microscope (WaveFX spinning disk confocal system, Quorum Technologies) and signals were quantified using Volocity 6.3 imaging software (PerkinElmer). Samples for β (1,3)-glucan analysis were treated identically except that the monoclonal antibody was obtained from BioSupplies, Australia (mouse monoclonal antibody to β (1,3)-glucan) (IgG, Kappa Light; Cat. No. 400-2).

Chitin

Fungi on coverslips were incubated with 50 μ L of a chitin probe solution (TMR-Star Conjugated Chitin-binding Probe, a gift from New England Biolabs Ltd.) (20 μ g/mL in PBS)

overnight in the dark at 4°C. Coverslips were rinsed with PBS, dried and processed as described for α (1,3)-glucan staining. Fluorescence was visualized on a spinning disk confocal microscope (WaveFX spinning disk confocal system, Quorum Technologies) and signals were quantified using Volocity 6.3 imaging software (PerkinElmer). For each strain/polysaccharide, at least 30 images were analyzed and exposure was controlled manually at 900 ms. Control samples were processed in parallel except that the primary antibody or chitin probe was not added.

Transmission Electron Microscopy (TEM)

Petri dishes containing YAG agar or YAG + 1M sorbitol agar were prepared and overlaid with a sterile disk of cellophane. Conidia of the appropriate fungal strain (1×10^6) were spread evenly over the surface of the cellophane. Each plate was incubated at 30°C for 20 h than at 37°C for 5 h and flooded with a fixative solution containing 2.5% EM-grade glutaraldehyde in 0.1 M sodium cacodylate buffer, pH 7.4. Plates were incubated at room temperature for 1 h, washed with sodium cacodylate buffer and a 1-cm² piece of cellophane was transferred to a microcentrifuge tube filled with 0.1 sodium cacodylate buffer. Samples were dehydrated in an ethanol series, followed by 1:1 solution of ethanol/propylene oxide (1:1) then pure propylene oxide. The samples were soaked in a series of propylene oxide/Spurr resin mixtures (3:1, 1:1, 1:3, 0:1). Each sample was incubated in 100% resin for 2 days with resin replaced twice each day. Resin was polymerized at 70°C for 8 h. Samples were examined on a Hitachi H-7600 transmission electron microscope. From the TEM images of hyphae, cell wall thickness was quantified with ImageJ using the measure function. A random number generator produced 5 sets of x,y co-ordinates for each image. ImageJ was used to locate coordinates and measure the thickness of the cell wall directly across using the measurement tool (calibrated to each scale bar). If the chosen co-ordinate was not on the cell wall, the line tool was used to find the shortest straight line to the cell wall, and the wall measurement was made at that point where the angle of intersection with each side of the cell wall as close to 90 degrees as possible. Measurements were performed blinded on coded images. The number of separate images analyzed for each condition was as follows: WT (17), Δ kdnase (17), WT + 1M sorbitol (12), Δ kdnase + 1 M sorbitol (24).

Scanning Electron Microscopy

Conidia (5×10^6) from each strain were incubated in RPMI 1640 overnight at 37°C on sterile round coverslips (25 mm). RPMI was replaced with 3 mL of a solution containing 0.075% Alcian Blue, 75 mM lysine, 3% glutaraldehyde in 0.1 M sodium cacodylate buffer, pH 7.2 and further incubated at 4°C overnight. Addition of Alcian Blue and lysine have been shown to enhance visualization of the polyanionic exopolysaccharides (Fischer et al., 2005). Samples were washed 3 times each with 0.1 M sodium cacodylate buffer, pH 7.2, and distilled water. After dehydration in ethanol (25, 50, 75, 90, 100, and 100% for 10 min each), samples were critical point dried, coated with iridium (5 ± 1 nm) and examined on a Nova NanoSEM (FEI).

Neutropenic Mouse Model of Invasive Aspergillosis

All experiments were carried out in accordance with the Canadian Council on Animal Care (CCAC) guidelines. This study was approved by the University Animal Care Committee at Simon Fraser University (protocol 1193B-11). The mouse model of pulmonary IA was modified from (Dixon et al., 1989). Briefly, female BALB/cJ mice (~3 months of age) from Jackson Laboratory (Bar Harbor, ME, United States) were acclimatized for 2 weeks prior to experimentation. Mice were immunocompromised with intraperitoneal injections of 0.025 g/ml cyclophosphamide (Toronto Research Chemicals, North York, ON, Canada) in PBS (100 mg/kg) administered on day 4 and day 0, and subcutaneous injections of 0.05 g/mL cortisone acetate (Sigma–Aldrich Canada Co., Oakville, ON, Canada) in PBST (200 mg/kg) on day 1. Experimental groups were inoculated intranasally with 1.0×10^6 fungal spores in 40 μ L aliquots, as follows: seven mice received wild type *Aspergillus fumigatus* spores, seven mice received wild type *Aspergillus fumigatus* spores followed by a dose of 5 mg/kg of liposomal amphotericin B (AmBisome) (AB) (Gilead Sciences Inc., Foster City, CA, United States), seven mice received Δ kdnase *A. fumigatus* spores, seven mice received Δ kdnase *A. fumigatus* spores and 5 mg/kg AB, seven mice received Δ kdnase^R strain *A. fumigatus* spores, three mice received saline, and four mice received saline and 5 mg/kg AB. AB was administered 4 h after spore inoculation on day 0; the drug was resuspended in water just prior to use, and administered intravenously.

Mice were maintained in a specific pathogen-free facility, four to a cage, with alternating 12-h light schedules. Mice were housed in autoclaved cages and received irradiated chow *ad libitum* (equal parts mixture of PicoLab Mouse Diet 20 and PicoLab Rodent Diet 20). Mice were provided with a tetracycline water (0.5 g/L) mixture sweetened with aspartame (Sigma–Aldrich Canada Co., Oakville, ON, Canada). Mice were monitored and weighed daily. At experimental end-points (>20% weight loss, swelling around the eyes, piloerection, hunched posture, limited mobility and activity, rapid breathing or gasping, and antisocial behavior), mice were humanely euthanized by CO₂ followed by removal of lungs. After euthanasia, perfusion with ice cold PBS was performed to clear blood from mouse lungs. The left lobe was fixed overnight at 4°C in paraformaldehyde, then transferred to an ethanol solution, and prepared for histology. The right lobe was split into two, one section was stored in TRIzol (Invitrogen) at 4°C for cytokine analysis via qPCR, the other section was frozen in a pre-weighed bag at –20°C for DNA analysis for fungal burden.

Lung Histology

Fixed lungs were sectioned and stained with hematoxylin and eosin (H&E) or with Grocott's methenamine silver (GMS) to visualize fungal elements (hyphae and conidia). Fungal elements were quantified as total fungal element area using the color threshold tool in ImageJ on GMS-stained sections, and expressed as percent fungal element coverage of total lung area.

Quantification of Macrophages and Neutrophils Cells in Fixed Lung Sections

Lung sections (4 μ m thick) were de-paraffinized with 3 xylene washes and re-hydrated by successive washes in 100, 90, and 70% ethanol, and then finally in dH₂O. Heat-based antigen retrieval was performed by heating slides in citrate buffer (pH 6.0) to 120°C in a pressure cooker. Slides were then incubated with 5% donkey serum for 30 min and endogenous peroxidase was inhibited with 0.3% H₂O₂ treatment for 20 min. Slides were incubated with the primary antibody overnight, the biotinylated secondary antibody for 30 min, and horseradish peroxidase-conjugated avidin-biotin complex (Vector Laboratories, Burlingame, CA, United States) for 45 min. Staining was visualized with 3-amino-9-ethyl carbazole (AEC) substrate chromagen, which results in red staining (Vector Laboratories). Sections were then counterstained with hematoxylin. The following primary antibodies were used: Mac-3 (5 μ g/mL) (BD Biosciences, Franklin Lakes, NJ, United States) to visualize macrophages and myeloperoxidase (MPO) to visualize neutrophils (5 μ g/mL) (Abcam, Cambridge, MA, United States). Immune cells were manually counted on a microscope. Quantification of the staining was performed in a manner that was blinded from knowledge of specific mouse IDs. The total lung area for each section was quantified in ImageJ and Mac-3-positive or MPO-positive cells were expressed per total area (mm²).

Fungal Burden Analysis by qPCR

Analysis was based on the method of Bowman et al. (2001). Frozen lung samples in pre-weighed bags were minced and homogenized in cold saline (7.5 volumes/g lung) using a roller bottle, and transferred to microcentrifuge tubes. Secondary homogenization was carried out in a TissueLyser II (3 sets of 30 s at 30 oscillations/s) and centrifuged for 5 min at 800g and 4°C. Genomic DNA was extracted using the CTAB method (Carlson et al., 1991) and fungal DNA was amplified by TaqMan quantitative PCR (Life Technologies). We targeted the internal transcribed spacer region, ITS1 and the 5.8S gene located between the 18S and 28S rRNA genes, using the following primers: Forward Primer - TCTGAAAGTATGCAGTCTGAGTTGATT; Reverse Primer - GATGCCGGAACCAAGAGATC; Probe - CGTAATCAGTTAAACTTTC. A *C_t* value was determined for triplicates from each sample, based on a standard curve also created using triplicate samples with genomic DNA from *A. fumigatus* (0.001–1.000 ng/ μ L).

Interaction of Conidia with J774 Mouse Macrophages

To determine the proportion of conidia internalized by macrophages, we labeled conidia with fluorescein isothiocyanate (FITC) (470 nm). Bound/external conidia were detected by an anti-*Aspergillus* antibody conjugated to a red fluorophore (590 nm) added to the cell suspension at the end of the incubation period. All strains were grown on YAG media supplemented with appropriate antibiotics (100 μ g/mL hygromycin for the Δ kdnase strain and 50 μ g/mL phleomycin for Δ kdnase^R) for

72 h at 37°C and harvested in PBST as described above. To label conidia with FITC, we followed the procedure of Sturtevant and Latge (1992). The J774A.1 cell mouse macrophage cell line, originally derived from BALB/cN mice (ATCC, Manassas, VA, United States) were grown on coverslips in 24-well plates in RPMI 1640 media containing 10% fetal bovine serum (RPMI-FBS). Macrophages (2.5×10^5 cells) were incubated at 37°C + 5% CO₂ for 3 h and blocked in RPMI-FBS containing 0.5% BSA for 1 h at 37°C. The medium was aspirated and FITC-labeled conidia from each strain (2×10^6 , suspended in 1 mL RPMI-FBS) were added to the wells. Each strain was inoculated into separate wells and no spore control and no primary antibody control wells were also included. Plates were incubated for 1 h at 37°C in 5% CO₂ then placed on ice. On ice, J774 cells were washed 3× with PBST and incubated for 1 h with a 1:75 dilution of polyclonal rabbit anti-*Aspergillus* cell wall antibody (Wasylnka and Moore, 2002) in PBS plus 10% goat serum (GS). After washing 3 times, Alexa Fluor 594-conjugated AffiniPure goat anti-rabbit IgG (H+L) (Jackson ImmunoResearch) was added in 1:575 dilution in PBS-GS. After incubation for 1 h, cells were washed with PBS and fixed in PBS-4% formalin for 1 h. Washed coverslips were mounted with Prolong Antifade Mounting Media, sealed and stored in the dark at 4°C. Images were obtained a Zeiss Axioplan epifluorescence microscope.

Macrophage killing of conidia was measured *in vitro* using the nystatin protection assay (Wasylnka and Moore, 2002), except that J774A.1 cells were incubated in RPMI-FBS containing 0, 10, or 20 µg/mL hydrocortisone dissolved in DMSO for 24 h prior to adding conidia. Control samples were treated with DMSO.

RESULTS

Deletion of the *A. fumigatus* Kdnase

The *kdnase* gene on chromosome 4 was disrupted by *Agrobacterium*-mediated transformation of *A. fumigatus*

using a fusion PCR construct that contained a hygromycin resistance cassette for positive selection flanked by 1000 bp *kdnase* up- and downstream sequences (Supplementary Figure S1). Successful generation of a $\Delta kdnase$ strain was determined by PCR and Southern blotting. The Southern blot confirmed homologous insertion of the knockout construct at the *kdnase* locus (Supplementary Figure S2). The complemented mutant, $\Delta kdnase^R$ or 'rescued' strain, was produced by electroporation of the knockout with the wild type (WT) *kdnase* gene controlled by its native promoter (928 bp of upstream sequence). Successful *kdnase* knockout and ectopic insertion of the WT *kdnase* gene into the genome of the $\Delta kdnase$ strain was confirmed by PCR (Supplementary Figure S3).

Comparative Growth of Wild Type and $\Delta kdnase$ Strains on Minimal Media Supplemented with Varying Carbon Sources

A growth assay was performed to determine how the loss of the *kdnase* gene affected the nutritional requirements of *A. fumigatus*. Strains were grown for 72 h on Kafer's minimal medium containing only the specified carbon source. When grown on minimal media supplemented with Kdn, glucose, or mannose, the growth of the $\Delta kdnase$ strain was inhibited compared to WT (Figure 1). Compared to Kdn, Neu5Ac (labeled sialic acid in Figure 1) is a poor carbon source for *A. fumigatus*; however, the $\Delta kdnase$ strain had even lower growth than WT on Neu5Ac. These data also confirm our previous finding that Kdn is strongly preferred to Neu5Ac in *A. fumigatus* (Telford et al., 2011).

Sorbitol Inhibits the Growth of the $\Delta kdnase$ Strain

We examined the relative growth and morphology of the WT and mutant strains in the presence of a hyperosmotic

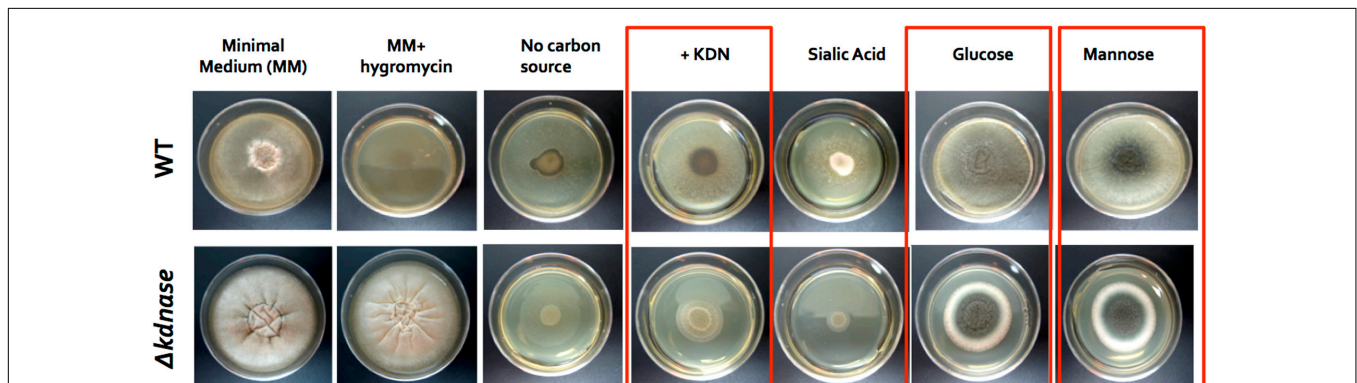
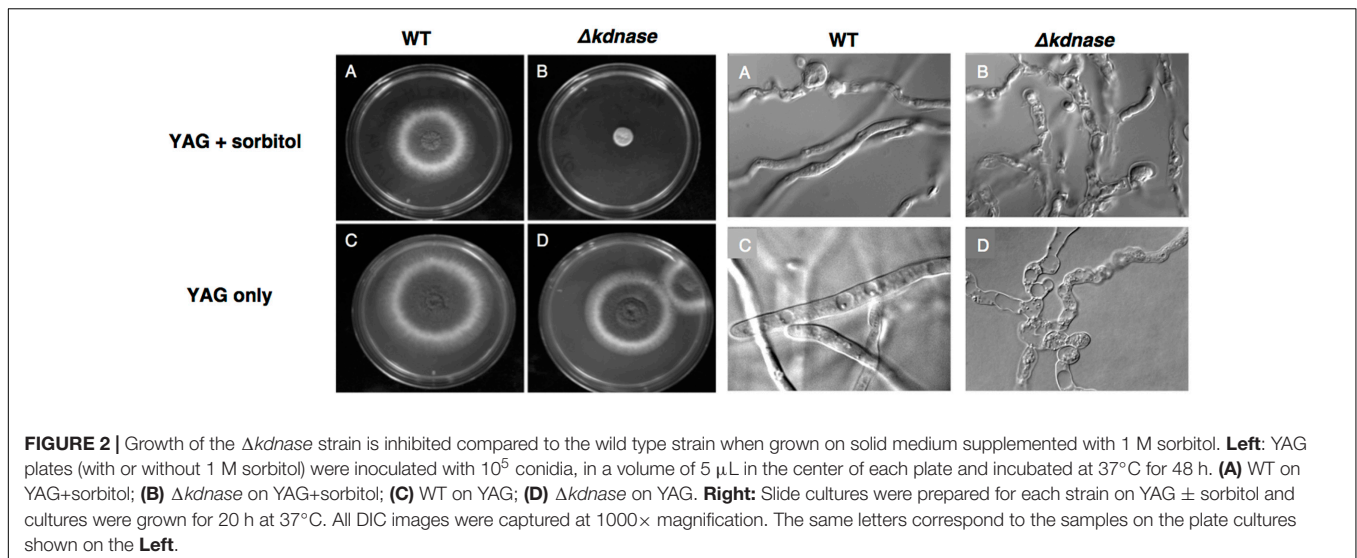


FIGURE 1 | Comparative growth of wild type and $\Delta kdnase$ strains on minimal media supplemented with varying carbon sources. Wild type and $\Delta kdnase$ strains were plated on solid Kafer's minimal medium (fungal media), supplemented with various carbon sources. Sialic acid is *N*-acetylneuraminic acid (Neu5Ac). Equivalent numbers of conidia were inoculated into the center of each plate and plates were incubated for 72 h at 37°C. Growth differences between the parental strain and the knockout are noted with boxes. Hygromycin resistance is the $\Delta kdnase$ selectable marker and the mutant but not the wild type grew in the presence of hygromycin, as expected. Three other $\Delta kdnase$ mutants displayed the same phenotype (data not shown).



stress generated by addition of 1 M sorbitol to rich medium (YAG). Growth of the WT and $\Delta kdnase$ strains was similar on solid YAG medium although the morphology of the KO strain was abnormal. However, the $\Delta kdnase$ strain showed poor growth on YAG supplemented with sorbitol (Figure 2). A dose response experiment showed that growth inhibition was evident at concentrations of sorbitol of 0.4 M (data not shown). DIC images of slide cultures of the two strains showed that the morphology of the $\Delta kdnase$ hyphae was abnormal even in YAG alone with hyperbranching and swollen filaments (Figure 2 and Supplementary Figure S4). Quantitative analysis in RPMI-sorbitol medium showed that growth of the KO strain was <10% of WT after 48 h though some recovery was evident after 72 h (Supplementary Figure S4).

Deletion of *kdnase* Alters *A. fumigatus* Ultrastructure and Causes Compensatory Cell Wall Thickening under Hyperosmotic Stress

We examined the surface structure of conidia and hyphae of the WT, $\Delta kdnase$, and $\Delta kdnase^R$ strains grown in RPMI using scanning electron microscopy. No apparent structural changes in conidia were evident (data not shown); however, $\Delta kdnase$ hyphae had a less dense glycocalyx, a structure that is principally composed of polyanionic exo-polysaccharides. The rescued strain had an intermediate phenotype (Supplementary Figure S6). We quantified galactosaminogalactan (GAG) content of the three strains using lectin staining [soybean agglutinin (SBA) linked to a fluorophore] but found no significant differences (data not shown). Hence, changes in surface structure in the knockout cannot be attributed to alterations in GAG content. TEM images of hyphae showed that the cell walls of the $\Delta kdnase$ hyphae (panels A–D in Figure 3A) appeared thicker than those of WT (panels E–H in Figure 3A) when strains were grown in medium supplemented with sorbitol (compare panels C,D with panels G,H); this was confirmed by quantitative

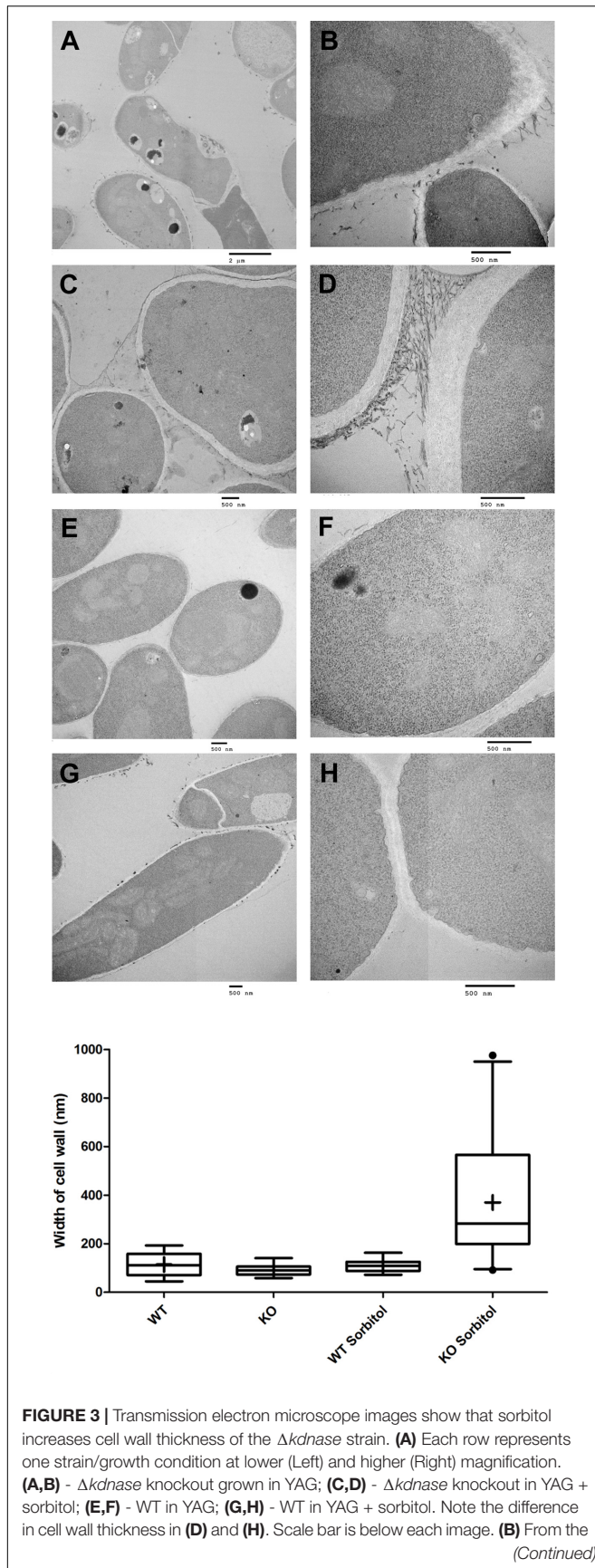
analysis of the images (Figure 3B). These data suggest that compensatory cell wall thickening occurred in response to the hyperosmotic stress in the $\Delta kdnase$ strain but not the WT strain.

The $\Delta kdnase$ Strain Is Resistant to the Growth Inhibitory Effects of Congo Red and Calcofluor White

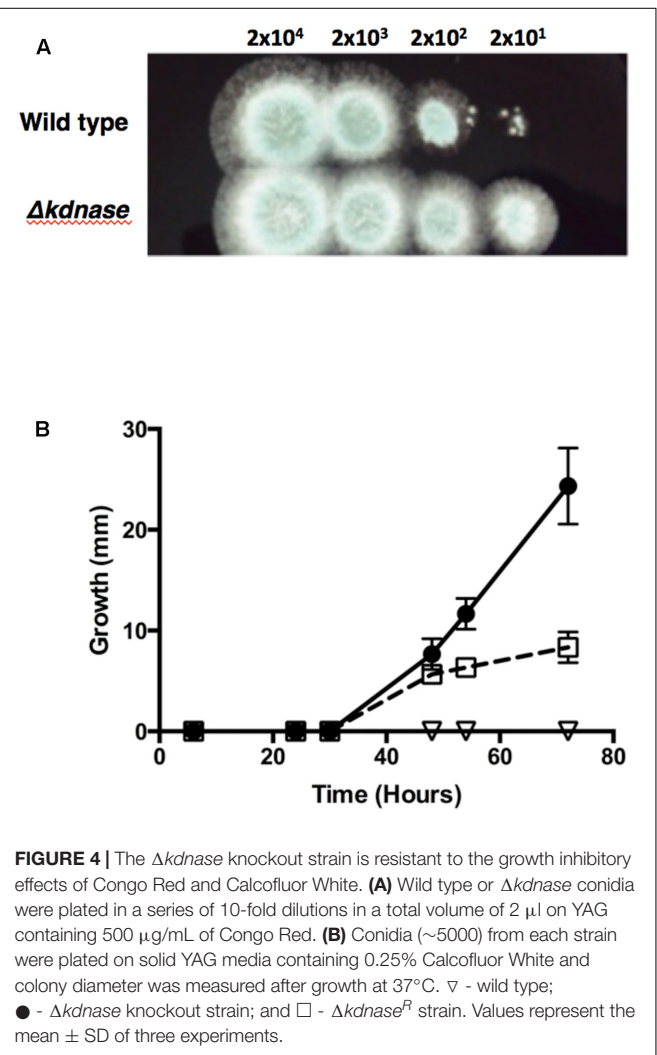
Chitin is an important structural polysaccharide of the *A. fumigatus* cell wall (Lee and Sheppard, 2016) and its synthesis is upregulated under conditions of cell wall stress. The dyes Congo Red (CR) and Calcofluor White (CW) were used to probe changes in the cell wall chitin content as these dyes bind structural polysaccharides with a preference for chitin (Roncero and Duran, 1985). Figure 4A and Supplementary Figure S5 show that the $\Delta kdnase$ strain was able to grow in concentrations of CR that almost completely inhibited WT growth on solid media. The rescued strain had an intermediate phenotype. The results with CW were similar: After 72 h of growth on YAG supplemented with 0.25% CW, the WT strain showed no growth whereas the $\Delta kdnase$ strain reached ~25 mm of radial growth. The $\Delta kdnase^R$ strain grew to only 30% of the level of the *kdnase* knockout strain (Figure 4B).

Hyperosmotic Stress Increases Cell Wall $\alpha(1,3)$ -Glucan and Chitin Levels in the $\Delta kdnase$ Strain

To directly quantify the levels of selected cell wall polysaccharides, strains were grown in slide culture on YAG medium with or without sorbitol (1 M) and immunofluorescence microscopy was used to measure the $\beta(1,3)$ -glucan, $\alpha(1,3)$ -glucan and chitin contents of the hyphae. Figure 5 shows that although no differences were detected in $\beta(1,3)$ -glucan, $\alpha(1,3)$ -glucan reactivity was significantly increased in $\Delta kdnase$ hyphae in the presence or absence of sorbitol by approximately 30% (Figures 5A,B). Binding of the chitin probe was dramatically

**FIGURE 3 |** Continued

TEM images of hyphae, cell wall thickness was quantified with ImageJ using the measure function. Cell wall thickness was measured 5 times in each image at coordinates determined by random number generation. The number of separate images analyzed for each condition is as follows: WT – 17, *Δkdnase* (KO) – 17, WT + 1M sorbitol – 12, *Δkdnase* + 1M sorbitol – 24. Whiskers represent the 5–95% confidence interval, the dots indicate outliers, and the + indicates the median. The KO plus sorbitol group was significantly different from all other groups at $p < 0.001$ (ANOVA followed by multiple comparison test with the Bonferroni correction).



different in the three strains; the *Δkdnase* strain grown in sorbitol had a threefold higher level of fluorescence compared to all other strains and conditions (Figure 5C and Supplementary Figure S7). These data suggest that resistance to CR and CW and the observed cell wall thickening in hyperosmotic conditions may be a consequence of increased chitin deposition in the cell wall of the *Δkdnase* strain. Alternatively, the increased fluorescence may reflect increased access of the probe to chitin as a consequence of cell wall disorganization in the *Δkdnase* strain.

Susceptibility to Various Antifungal Agents

We next tested the relative susceptibility to several antifungal agents. Nikkomycin Z is a competitive inhibitor of chitin synthase (Hector, 1993). The $\Delta kdnase$ strain was more resistant to nikkomycin than WT (Figure 6A) even though WT *A. fumigatus* strains already have high minimum inhibitory concentration values for nikkomycin (16–64 $\mu\text{g}/\text{mL}$) that limit its clinical use (Ganesan et al., 2004). The $\Delta kdnase$ strain also showed some resistance to voriconazole, a drug that alters membrane sterol composition by inhibiting cytochrome P450 lanosterol demethylase (Odds et al., 2003), but resistance was only detected in a narrow voriconazole concentration (Figure 6B). We did not detect a difference in the susceptibility of the $\Delta kdnase$ strain to itraconazole, another triazole antifungal (data not shown). In contrast, $\Delta kdnase$ was more susceptible than WT to both caspofungin and amphotericin B (Figures 6C,D). Caspofungin is an echinocandin antifungal that inhibits the Fks1 subunit of $\beta(1,3)$ -glucan synthase (Odds et al., 2003). It is the only anti-fungal agent that directly targets the cell wall. At caspofungin concentrations $<1 \mu\text{g}/\text{mL}$, no difference in growth was observed between the two strains (data not shown); however, at $>5 \mu\text{g}/\text{mL}$ caspofungin (concentrations at which ‘paradoxical’ growth occurs), $\Delta kdnase$ growth was marginally, but significantly, reduced compared to the WT strain (Figure 6). Finally, $\Delta kdnase$ also showed increased sensitivity to Amphotericin B (AB) compared to WT (~ 6 -fold at 0.7–0.8 $\mu\text{g}/\text{mL}$) (Figure 6). AB is a pore-forming polyene antibiotic used as an alternative to voriconazole in primary treatment of IA. Because of the clinical importance of AB and the *in vitro* sensitivity of the $\Delta kdnase$ knockout strain, we included AB treatment in our test of *Af* $\Delta kdnase$ virulence.

The $\Delta kdnase$ Strain Has Reduced Virulence and Fungal Burden in Combination with Amphotericin B Treatment in a Neutropenic Mouse Model of Invasive Aspergillosis

To test the virulence of the $\Delta kdnase$ knockout strain and the efficacy of AB treatment *in vivo*, female BALB/c mice were first immunosuppressed with cortisone and cyclophosphamide as described in the Section “Materials and Methods.” On day 0, mice in all treatment groups (seven per group) received 10^6 conidia intranasally of the appropriate strain. Two groups of animals were also treated with AmBisome (AB) (5 mg/kg i.v.) 4 h after exposure to $\Delta kdnase$ (KO), or $\Delta kdnase^R$ (R) conidia. Two additional groups of control mice received the same immunosuppressive regime and were exposed to saline intranasally ($n = 3$) or saline followed by AB treatment ($n = 4$). Control mice (not infected with *A. fumigatus*) had 100% survival (data not shown). Kaplan-Meier survival curves of immunosuppressed mice exposed to wild type (WT), $\Delta kdnase$ (KO), or $\Delta kdnase^R$ (R) conidia with or without AmBisome treatment are shown in Figure 7. All mice were weighed and monitored by a blinded observer twice per day for up

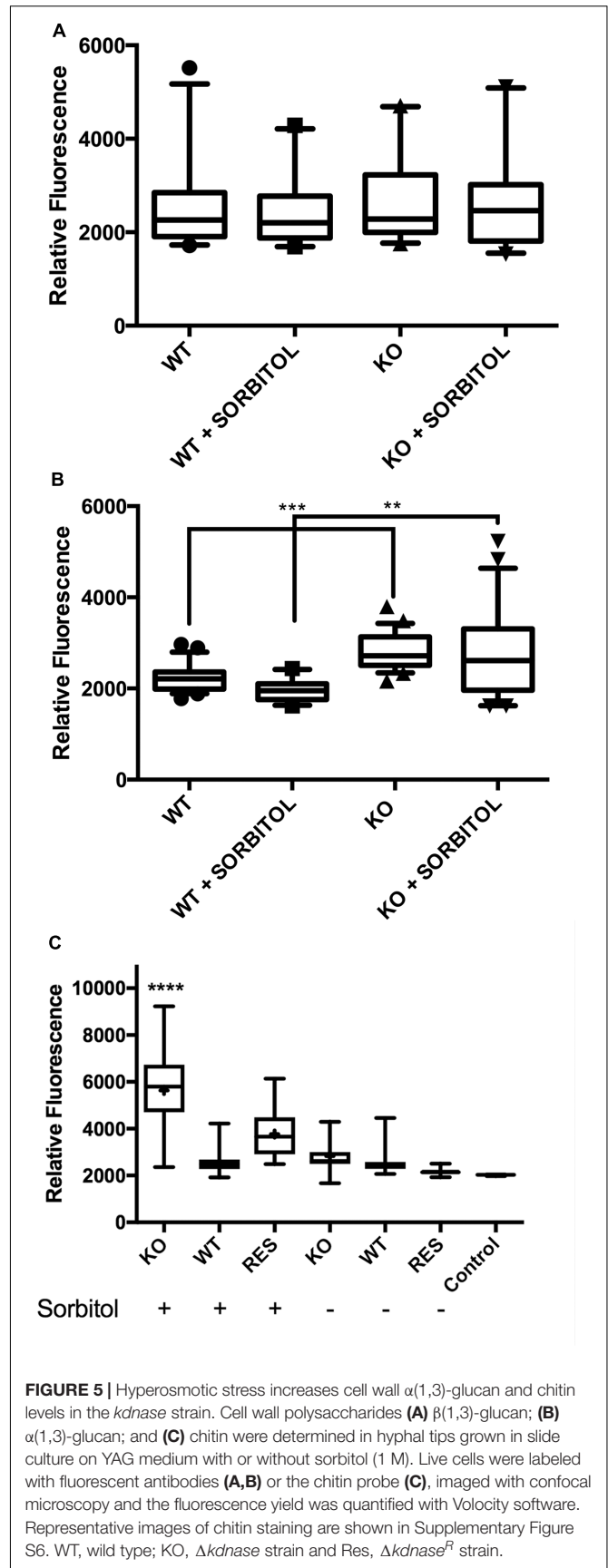
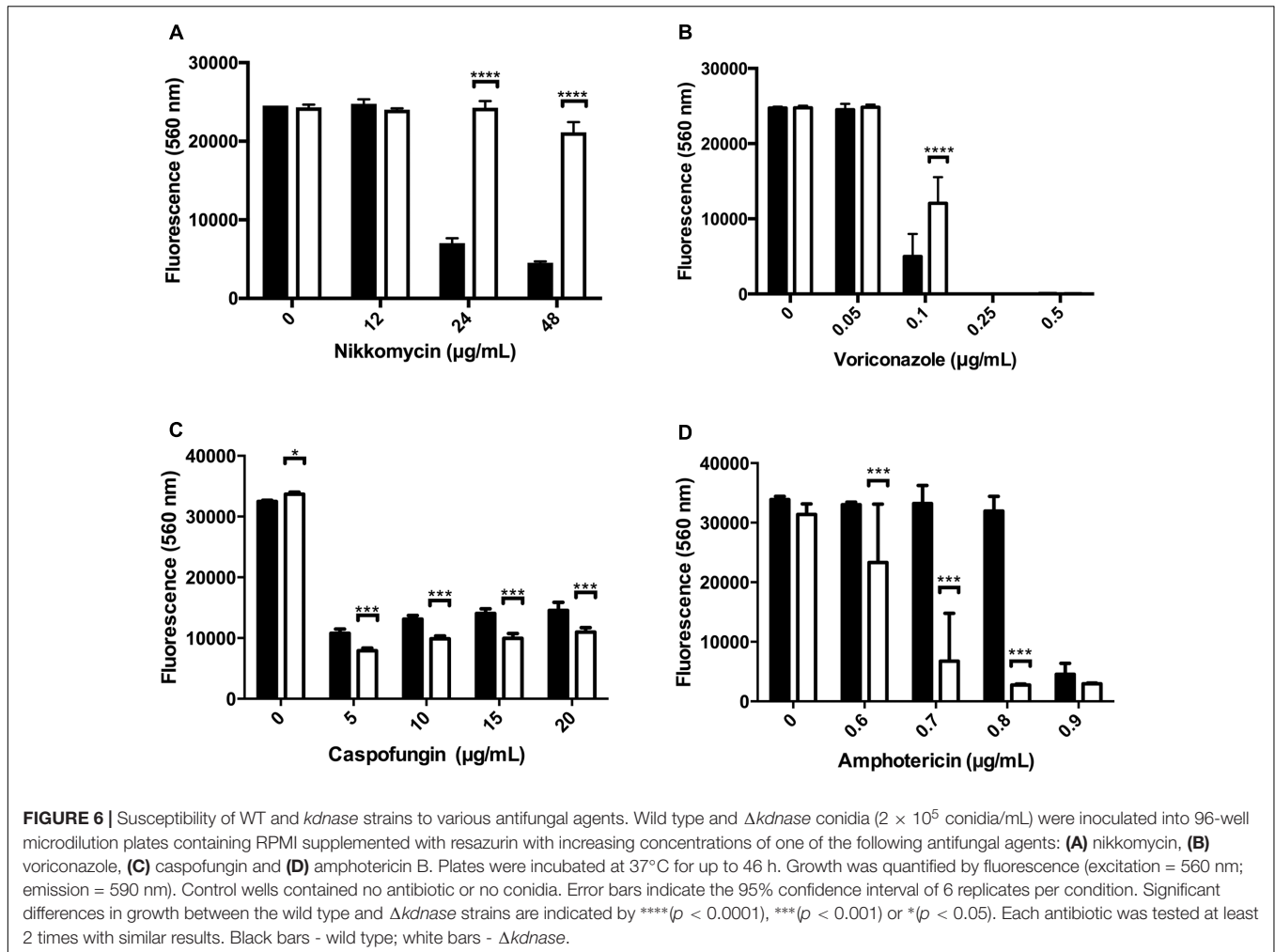


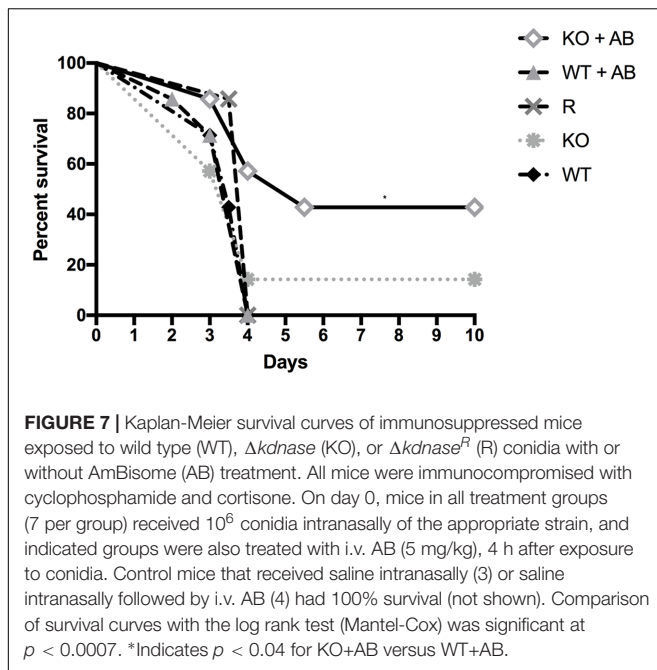
FIGURE 5 | Hyperosmotic stress increases cell wall $\alpha(1,3)$ -glucan and chitin levels in the *kdnase* strain. Cell wall polysaccharides (A) $\beta(1,3)$ -glucan; (B) $\alpha(1,3)$ -glucan; and (C) chitin were determined in hyphal tips grown in slide culture on YAG medium with or without sorbitol (1 M). Live cells were labeled with fluorescent antibodies (A,B) or the chitin probe (C), imaged with confocal microscopy and the fluorescence yield was quantified with Volocity software. Representative images of chitin staining are shown in Supplementary Figure S6. WT, wild type; KO, $\Delta kdnase$ strain and Res, $\Delta kdnase^R$ strain.



to 10 days (experimental endpoint): Mice showing signs of morbidity approaching a humane endpoint were sacrificed. Most mice reached a humane endpoint by day 4 with the exception of one infected with the $\Delta kdnase$ strain (KO) (1/7 survived) and four mice infected with the $\Delta kdnase$ strain that also received AmBisome treatment following spore exposure (KO+AB) (3/7 survived for 10 days). These surviving mice also gained weight and had no apparent symptoms (data not shown). Using the log rank test, a significant difference in survival was found ($p < 0.0007$). Comparison of KO+AB and WT+AB were significantly different at $p < 0.04$. Fungal burden at endpoint was assessed by two methods. Fungal DNA content was measured by qPCR and data were analyzed using a one-way ANOVA followed by a Games Howell test for differences between groups. The $\Delta kdnase$ plus AmBisome (KO+AB) cohort was the only group in which fungal burden was not statistically different from the controls (CON+AB), and the median fungal burden in the KO+AB treatment group was 10-fold lower than in WT+AB (Figure 8A). We also quantified fungal elements in 3 lung sections from each animal in the WT+AB ($n = 7$) and KO+AB ($n = 6$) treatment groups and the data are summarized in Figure 8B. The percent coverage of the lung by fungal elements in

GMS-stained lung sections corroborated the fungal DNA burden data: WT+AB mice had values ~10-fold higher than the KO+AB group. Thus, the increased susceptibility of the $\Delta kdnase$ strain to amphotericin B we observed *in vitro* (Figure 6) was replicated *in vivo* and resulted in a lower fungal burden and greater survival of the host in the KO+AB group.

Exposure to the $\Delta kdnase$ strain resulted in a significantly lower lung fungal burden compared to wild type with or without AmBisome treatment, even in the animals that died from the disease. To determine whether the relative growth of the two strains may have contributed to this difference, we measured growth in minimal essential medium (MEM) supplemented with 15% human serum. After 18 and 25 h at 37°C, the $\Delta kdnase$ strain had approximately 50% of the growth of the WT strain but by 48 h, cell density was equivalent between the two strains (data not shown). Moreover, in the antibiotic sensitivity experiments after 28–48 h, the growth of WT and $\Delta kdnase$ strains were equivalent in the no antibiotic control samples (Figure 6). Finally, the data in Figure 7 show that mice exposed to the $\Delta kdnase$ strain without AB treatment did not survive longer than mice that were given the WT strain. We confirmed this in a separate mouse study in which we found that

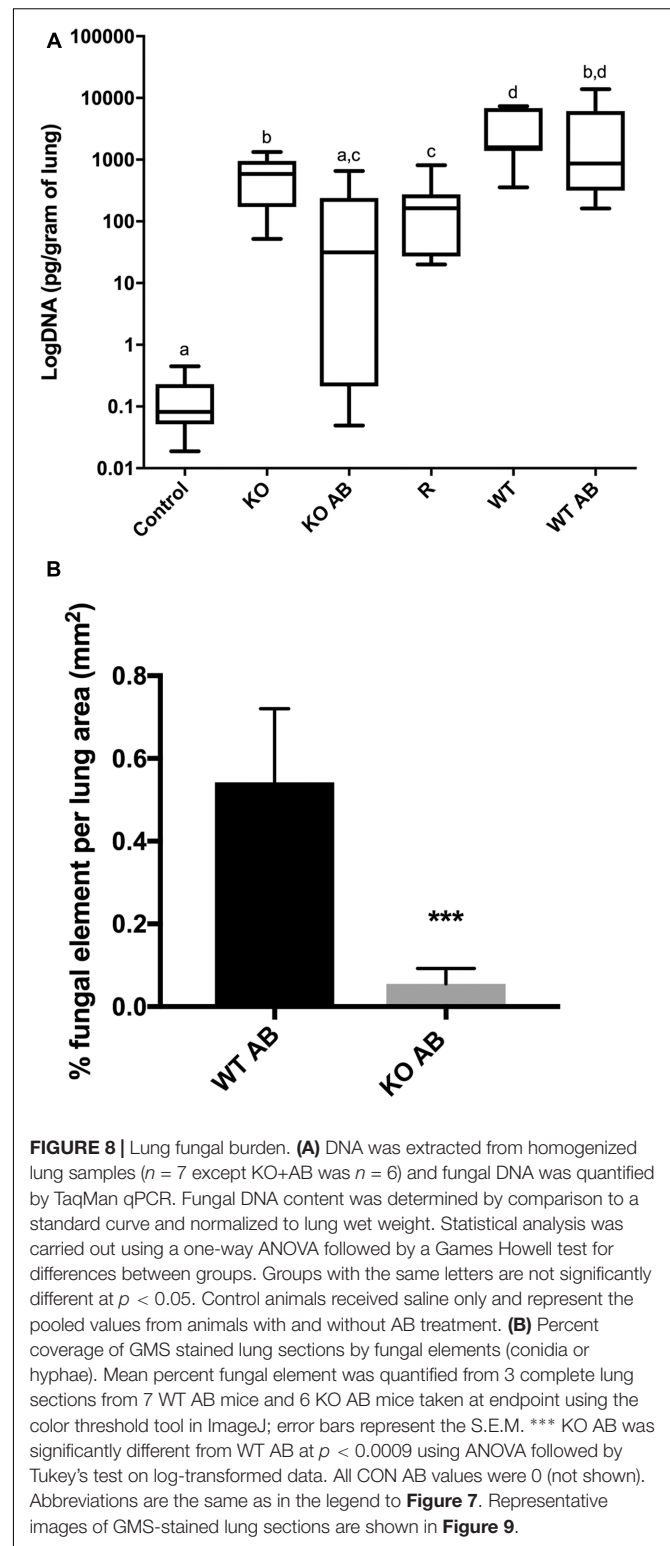


the survival of BALB/c female mice was the same in the WT or $\Delta kdnase$ treatment groups (data not shown). This suggests the combination of amphotericin B with $\Delta kdnase$ deletion was responsible for the lower fungal burden and increased survival.

Representative sections of H&E and GMS stained lung sections from AmBisome-treated animals are shown in **Figure 9**. Extensive cellular infiltrates and hemorrhage were evident in WT+AB group, and clusters of fungal filaments were abundant in lung sections. In the KO+AB mice, although inflammation and fungal elements were evident, these were more restricted in size and less frequently observed (**Figure 9**). GMS-stained sections from mice exposed to WT, $\Delta kdnase$, or $\Delta kdnase^R$ without AB treatment are shown in Supplementary Figure S8.

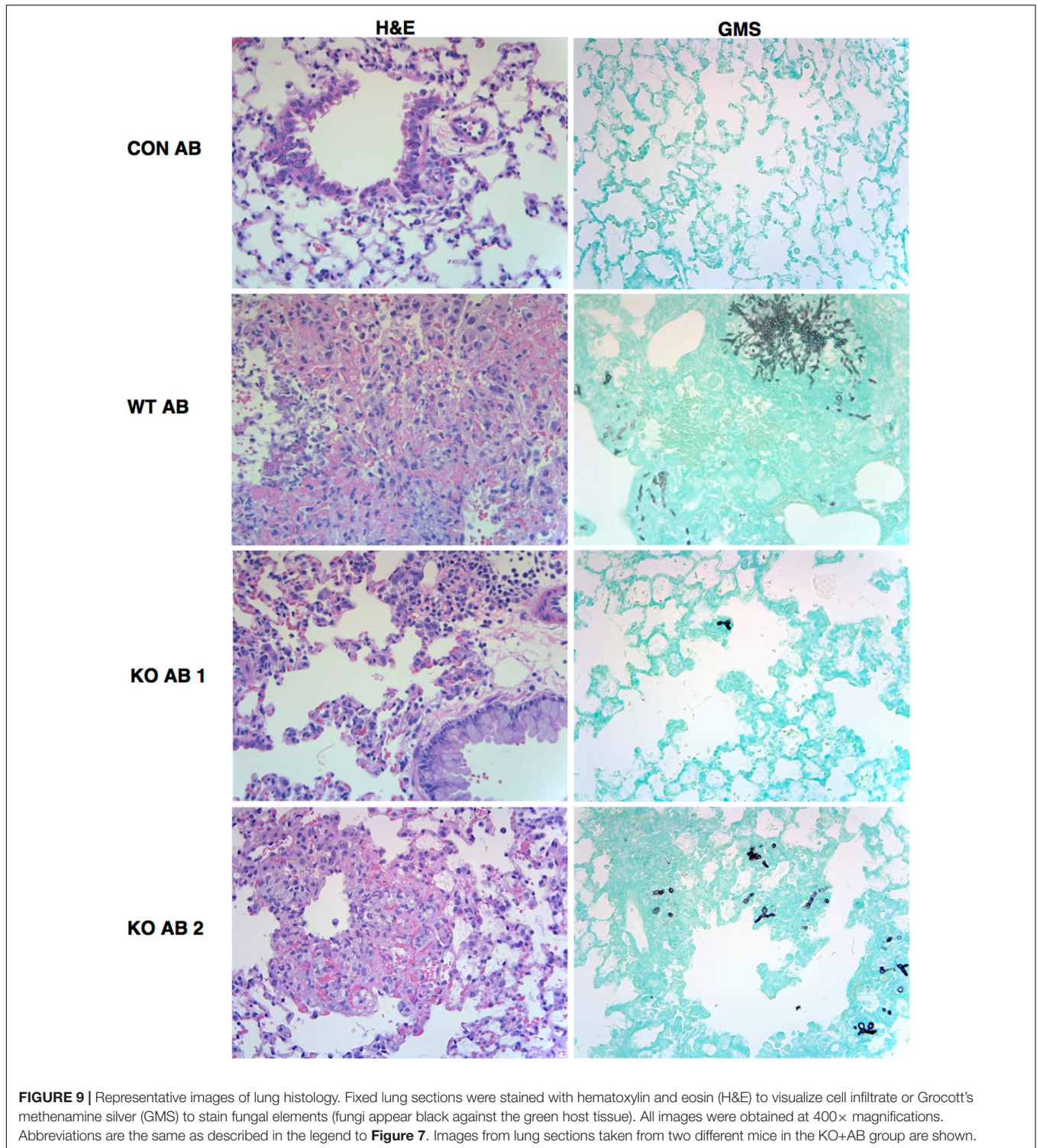
Leukocytes in Lung Sections

We examined the relative numbers of macrophages and neutrophils in lung sections from the AmBisome treatment groups at endpoint using immunohistochemistry. Neutrophil (MPO-positive cells) counts/ mm^2 in the lung of animals that received either WT or $\Delta kdnase$ conidia were elevated threefold over controls (**Figure 10A**); no significant difference was observed between the treatment groups. Macrophages (Mac 3-positive cells) were higher than control animals for both groups receiving *A. fumigatus*; however, the accumulation of macrophages detected in tissues of mice exposed to WT conidia was significantly lower than in $\Delta kdnase$ -exposed mice (**Figure 10B**). Supplementary Figure S9 contains representative photomicrographs showing the difference in the number and staining of the macrophages in a lung section from a mouse in the KO+AB group compared to one from WT+AB.



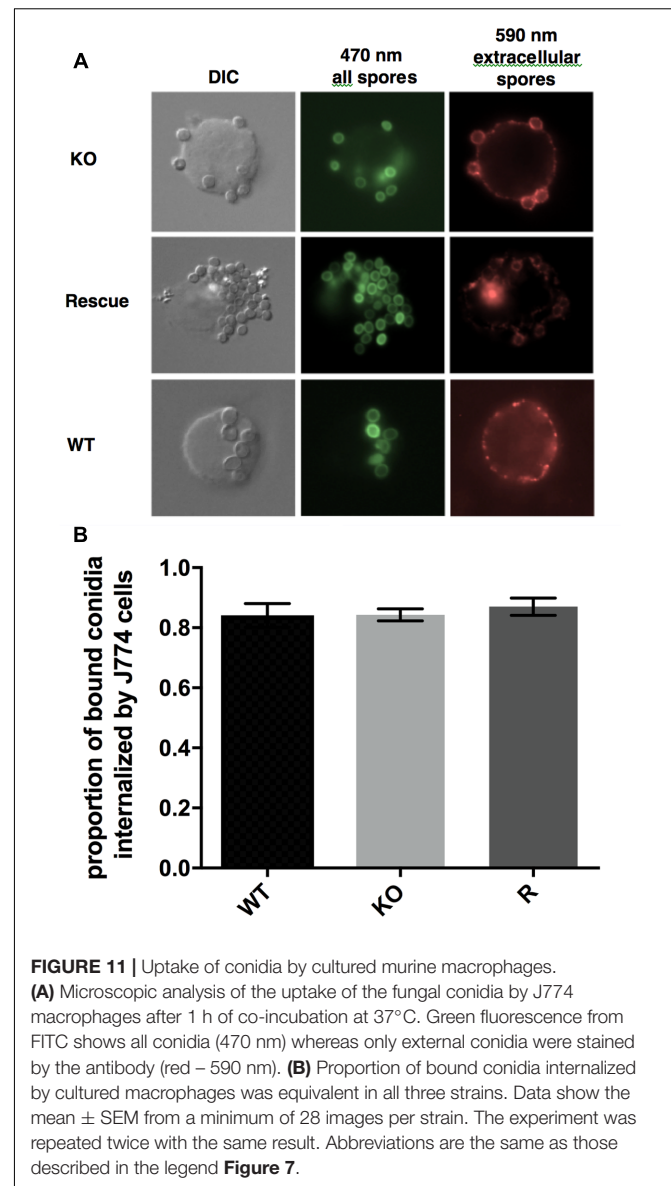
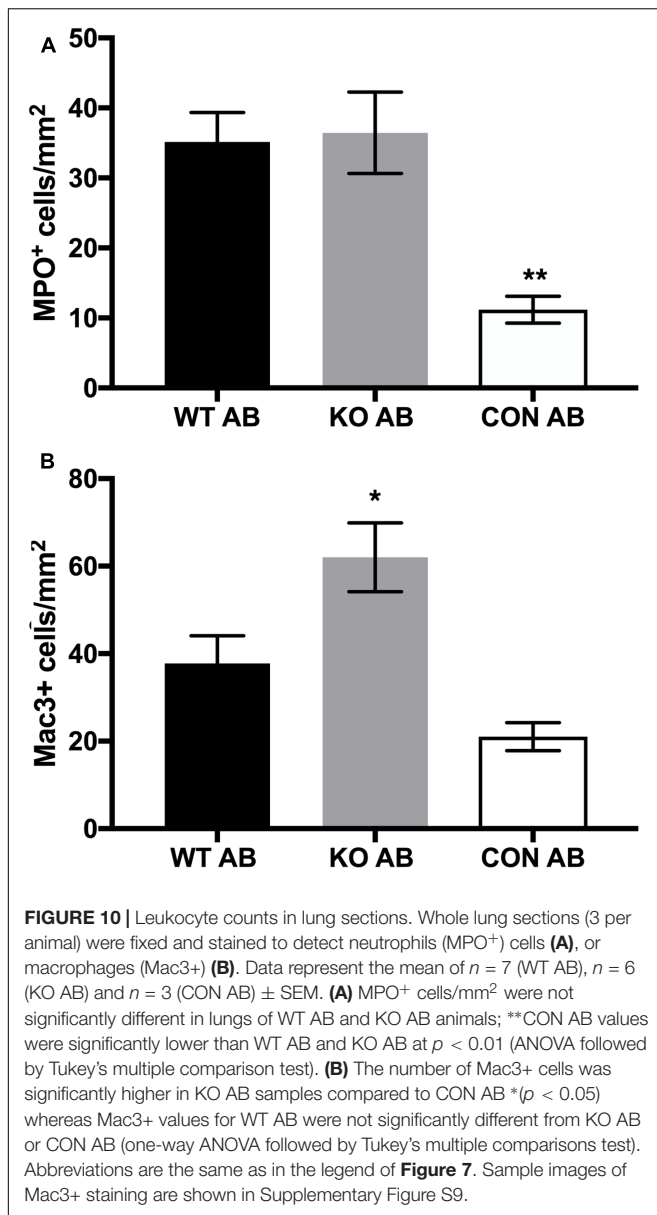
Uptake of Conidia by Cultured Murine Macrophages

Uptake and killing of conidia by macrophages is an important innate immune defense against *A. fumigatus*



(Philippe et al., 2003). We compared the uptake of FITC-labeled WT, $\Delta kdnase$, and $\Delta kdnase^R$ conidia, quantified with immunofluorescence microscopy in the cultured mouse macrophage cell line, J774. No difference in uptake by J774 cells was observed between the 3 strains (**Figure 11**) and a similar experiment that measured conidial uptake by

cultured human type 2 pneumocytes (A549 cells) produced the same result (data not shown). Thus, $\Delta kdnase$ conidia were internalized to the same extent as WT by both professional phagocytes and epithelial cells; however, whether there were differences in the rate of conidial killing was not determined.



DISCUSSION

Our study revealed an important role for the *Aspergillus fumigatus* sialidase (Kdnase) in maintaining hyphal cell wall stability in the presence of stressors such as hyperosmotic stress or selected antimicrobial agents. Deletion of *kdnase* increased the survival of mice that were treated with amphotericin B. To our knowledge, this is the first report that implicates a sialidase in cell wall homeostasis and virulence in fungi.

The *Aspergillus fumigatus* hyphal cell wall has an inner wall containing $\beta(1,3)$ -glucans, chitin, galactomannan (linked to chitin), galactosaminogalactan, and an outer cell wall composed of $\alpha(1,3)$ -glucans, galactomannan [covalently linked to $\beta(1,3)$ -glucan] covered in a loose sheath of galactosaminogalactan (Lee and Sheppard, 2016). Aberrant hyphal morphology and

excess chitin deposition were detected in the $\Delta kdnase$ knockout strain in response to cell wall stressors whereas $\beta(1,3)$ -glucan levels were unchanged. Upregulation of chitin synthesis in response to cell wall stress is a well-known phenomenon that involves the cell wall integrity (CWI) pathway suggesting that deletion of *kdnase* weakened the fungal cell wall. The CWI sensor proteins (WSC) are plasma membrane receptors that detect mechanical stress (Grice et al., 2013; Valiante et al., 2015) and are connected to the downstream mitogen-activate protein kinase (MpkA) cascade by the protein kinase C (PkcA). An *A. fumigatus* strain with a single amino acid substitution in PkcA (G579R), causing reduced Mpk-activating function, showed an increased sensitivity to CW, CR, and SDS, indicative of cell wall dysfunction (Rocha et al., 2015). The CWI pathway and the massive redundancy in some cell wall genes [e.g., *A. fumigatus* contains 8 chitin synthase genes (Muszkieta et al., 2014)] make

the cell wall a difficult therapeutic target; however, the targeting difficulty is outweighed by the cell wall's importance for fungal survival and the fact that the host lacks a cell wall.

Growth of the $\Delta kdnase$ strain was inhibited by hyperosmotic stress. In fungi, activation of the high osmolarity glycerol (HOG) pathway permits growth in hyperosmotic conditions, for example, by increasing expression of genes involved in glycerol biosynthesis (Bahn, 2008). Cross-talk between the CWI and the pathways is well established in *S. cerevisiae* (Fuchs and Mylonakis, 2009) and there is evidence from transcriptomic studies that they are also linked in *A. fumigatus* (Malavazi et al., 2009). The Type III hybrid histidine kinase, TscC both senses and signals downstream adaptation to prevent osmotic stress. The *A. fumigatus* $\Delta tscC$ mutant had a phenotype very similar to our $Af\Delta kdnase$ mutant including growth inhibition by sorbitol and resistance to Congo Red dye (McCormick et al., 2012). Interestingly, pharmacological activation of the HOG pathway in *A. fumigatus* with fludioxonil resulted in growth arrest and a remodeled hyphal cell wall, including increased deposition of chitin (Wiedemann et al., 2016). Further studies are required to determine whether the HOG pathway genes or gene products are altered in $\Delta kdnase$.

We were able to obtain only a partial rescue phenotype $\Delta kdnaseR$ despite attempting several strategies including ectopic insertion of *kdnase* with native promoter, ectopic insertion of *kdnase* with constitutive promoter, and homologous re-insertion of the gene at the correct locus. We also made a rescue construct containing the recently annotated 3' untranslated region (UTR); 3' UTR regions are known to regulate the translation, location and stability of mRNA transcripts (Mignone et al., 2002; Zhang and Sachs, 2015). However, no improvement of the rescued phenotype was observed (data not shown). Alternatively, epigenetics, or the environment surrounding the *kdnase* locus, could be responsible for the difficulty in achieving full complementation. Difficulty in producing a full rescue strain for a sialidase knockout mutant in *M. tuberculosis* was reported by May et al. (2012).

$Af\Delta kdnase$ was more sensitive than WT to caspofungin *in vitro*. Caspofungin is a lipo-peptide that inhibits $\beta(1,3)$ -glucan synthase resulting in growth arrest in *A. fumigatus*. However, at higher drug concentrations ($> 1 \mu\text{g/mL}$), caspofungin stimulates the growth of *A. fumigatus*, a phenomenon called the 'paradoxical effect' (Wiederhold, 2007). Fortwendel et al. (2010) showed that paradoxical growth was related to up-regulation of chitin synthesis via calcineurin signaling. In the $\Delta kdnase$ strain as with WT, growth increased at higher caspofungin concentrations, likely secondary to chitin synthesis, but growth of $\Delta kdnase$ was less than WT (Fortwendel et al., 2010). This suggests that, even with compensatory chitin deposition, the $\Delta kdnase$ strain was more susceptible to the effects of caspofungin on cell wall structure.

The $\Delta kdnase$ strain was also more sensitive to amphotericin B (AB) *in vitro* and *in vivo*. AB is a polyene anti-fungal agent and the first anti-fungal used clinically to treat IA (Mesa-Arango et al., 2012). Its mechanism of action is still unclear but involves pore formation in the plasma membrane upon hydrophobic interaction with ergosterol, the fungal membrane sterol (Urbina et al., 1987), as well as sterol sequestration (Palacios

et al., 2011; Gray et al., 2012) and induction of oxidative stress (Sangalli-Leite et al., 2011; Kim et al., 2012). Various studies have found a relationship between fungal cell wall patency and AB susceptibility. For example, the relative susceptibility of the *Kluyveromyces*, *Candida* and *Schizosaccharomyces* spp. to AB was correlated with cell wall chitin content but not to plasma membrane ergosterol content. Species or strains with high levels of chitin in their cell wall were shown to be more susceptible to challenge with amphotericin B (Bahmed et al., 2003). In the yeast pathogen, *Cryptococcus neoformans*, Banerjee et al. (2016) created a *ura1* Δ mutant lacking dihydroorotate dehydrogenase that showed both compromised cell wall structure and increased susceptibility to AB. They proposed that decreased nucleotide-sugar pools in the mutant resulted in structural defects in the cell wall that in turn, allowed a more rapid entry and greater binding of AB to the plasma membrane. Thus, the remodeling of cell wall structure that occurs during stress or in certain mutant strains such as $\Delta kdnase$ can lead to increased AB susceptibility.

The number of macrophages was significantly higher in KO+AB mice and this was positively correlated with survival ($R^2 = 0.73$). Alveolar monocyte recruitment into the mouse lung during inflammation is dependent on CCR2 (Maus et al., 2003) which is the receptor for the chemokine CCL2. Neutrophil and monocyte recruitment into the lung are interdependent so as to provide a coordinated inflammatory response during infection (Maus et al., 2003).

In vitro, the proportion of $\Delta kdnase$ and WT conidia internalized by J774 mouse macrophages was equivalent. This indicates that the fungal-specific pathogen-associated molecular patterns (PAMPs) in the $\Delta kdnase$ strain were recognized by macrophage pattern recognition receptors (PRRs). The C-type lectin receptors Dectin-1 and Dectin-2, and DC-SIGN bind fungal $\beta(1,3)$ -glucans, α -mannans and galactomannans, respectively (Erwig and Gow, 2016). Although we did not measure the galactomannan and mannan contents of the cell wall, $\beta(1,3)$ -glucan levels were unchanged in the $\Delta kdnase$ strain which may explain why we found no change in internalization. Many investigators have demonstrated that a small proportion of *A. fumigatus* conidia may germinate within the phagosome, effectively escaping from the cell (Schaffner et al., 1982; Wasylanka and Moore, 2003). Immune suppression by cortisone directly reduces the effectiveness of macrophage-mediated killing of *A. fumigatus*, allowing a greater proportion to escape (Schaffner et al., 1982). We hypothesize that the lower numbers of macrophages in the WT+AB mice may have been a consequence of macrophage destruction by germinating WT conidia although this needs to be confirmed experimentally.

To date, Kdn has been identified in relatively few organisms/tissues though its presence is likely underreported. It has been isolated from amphibian egg jelly coats (Strecker et al., 1992; Inoue and Kitajima, 2006), fish skin and reproductive tissues (Nadano et al., 1986; Kanamori et al., 1989; Song et al., 1991) and some bacteria (Shashkov et al., 2002; Ostash et al., 2014). In humans, only traces of Kdn were detected on glycoproteins and glycolipids present in the erythrocyte plasma membrane (Bulai et al., 2003). Interestingly, Kdn has

also been detected in human cancer tissue (Inoue et al., 1996, 1998). Preliminary evidence from our laboratory suggests that *A. fumigatus* may also contain Kdn (Zandberg et al., Unpublished results). Further study is required to precisely define the distribution and level of Kdn in the WT and $\Delta kdnase$ strains, and to determine whether Kdn is found in other fungi.

There is a large body of literature that clearly demonstrates the importance of sialidases in microbial virulence, particularly in bacteria. Much less is known about Kdnases and to our knowledge, other than in *A. fumigatus*, no other *kdnase* knockout strains have been constructed. The bacterium, *Sphingobacterium multivorum* has a Kdn-specific sialidase that, unlike *AfKdnase*, is incapable of using Neu5Ac as a substrate (Nishino et al., 1996). Predicted sialidase enzymes are present in other pathogenic *Aspergillus* species including *A. terreus*, *A. clavatus*, *A. sydowii*, and *A. lentulus* and in several dermatophytes; however, whether these are Kdnases has not been established. No Kdnase enzyme has been identified in any mammal. Humans express four sialidase isozymes, NEU1–NEU4, that differ in substrate specificity and tissue localization (Smutova et al., 2014). All human sialidases are inhibited by the sialidase transition state analog DANA (Neu5Ac2en) with IC₅₀ values that range from 6 to 90 μ M (Albohy et al., 2013). In contrast, we previously showed that Neu5Ac2en did not inhibit the recombinant *A. fumigatus* Kdnase even at concentrations up to 10 mM, but was inhibited by the related Kdn analog, 2,3-didehydro-2,3-dideoxy-D-glycero-D-galacto-non-2-ulonic acid (Kdn2en). Furthermore, Kdn2en bound to the enzyme in a 1.84 Å-resolution crystal structure (Telford et al., 2011). Thus, it is possible to selectively inhibit Kdnase without affecting host sialidases. Because humans do not express a Kdnase, a specific inhibitor of this enzyme would be expected to have a good safety profile. Small-molecule inhibitors of viral sialidases are already in clinical use including the two important anti-influenza drugs, zanamivir and oseltamivir (von Itzstein, 2007). Thus, inhibition of *Aspergillus fumigatus* Kdnase might have therapeutic potential for the treatment of IA, especially when combined with amphotericin B. Such a combination treatment strategy may allow for reduced amphotericin B dose and

accompanying toxicity. For this strategy to be successful, a small molecule Kdnase inhibitor must recapitulate the phenotype of the *kdnase* knockout.

AUTHOR CONTRIBUTIONS

Conceptualization: JN, ES, JY, and MM. Funding acquisition: MM and AB. Investigation: JN, ES, CS, AC, SM, JY, MH, and MM. Resources: MM, AB, JC, and KM. Visualization: JN, ES, CS, and MM. Writing – original draft: JN, ES, MH, AC, and MM. Writing – review and editing: JN, ES, JY, CS, AC, SM, AB, KM, JC, MH, and MM.

FUNDING

This research was supported by grants from the Natural Sciences and Engineering Research Council of Canada (MM) and the Canadian Glycomics Network (canadianglycomics.ca) (MM and AB).

ACKNOWLEDGMENTS

The authors thank New England Biolabs Inc. for their generous gift of the chitin probe. They are grateful to Ingrid Barta for assistance with histology, Bradford Ross and Dr. Matt Bilton for their guidance with electron microscopy as well as Natalie Kinloch, Gabriella Martine, Julia Mohr, Ashley Gilliland, Dr. Clive Roberts and Alison Hadwin for expert technical assistance.

SUPPLEMENTARY MATERIAL

The Supplementary Material for this article can be found online at: <https://www.frontiersin.org/articles/10.3389/fmicb.2017.02706/full#supplementary-material>

REFERENCES

- Albohy, A., Zhang, Y., Smutova, V., Pshezhetsky, A. V., and Cairo, C. W. (2013). Identification of selective nanomolar inhibitors of the human neuraminidase, NEU4. *ACS Med. Chem. Lett.* 4, 532–537. doi: 10.1021/ml400080t
- Alviano, C. S., Travassos, L. R., and Schauer, R. (1999). Sialic acids in fungi: a minireview *Glycoconj. J.* 16, 545–554. doi: 10.1023/A:1007078106280
- Arabyan, N., Park, D., Foutouhi, S., Weis, A. M., Huang, B. C., Williams, C. C., et al. (2016). *Salmonella* degrades the host glycocalyx leading to altered infection and glycan remodeling. *Sci. Rep.* 6:29525. doi: 10.1038/srep29525
- Bahmed, K., Bonaly, R., and Coulon, J. (2003). Relation between cell wall chitin content and susceptibility to amphotericin B in *Kluyveromyces*, *Candida* and *Schizosaccharomyces* species. *Res. Microbiol.* 154, 215–222. doi: 10.1016/S0923-2508(03)00049-4
- Bahn, Y. S. (2008). Master and commander in fungal pathogens: the two-component system and the HOG signaling pathway. *Eukaryot. Cell* 7, 2017–2036. doi: 10.1128/EC.00323-08
- Banerjee, D., Umland, T. C., and Panepinto, J. C. (2016). De novo pyrimidine biosynthesis connects cell integrity to amphotericin B susceptibility in *Cryptococcus neoformans*. *mSphere* 1:e00191-16. doi: 10.1128/mSphere.00191-16
- Bowman, J. C., Abruzzo, G. K., Anderson, J. W., Flattery, A. M., Gill, C. J., Pikounis, V. B., et al. (2001). Quantitative PCR assay to measure *Aspergillus fumigatus* burden in a murine model of disseminated aspergillosis: demonstration of efficacy of caspofungin acetate. *Antimicrob. Agents Chemother.* 45, 3474–3481. doi: 10.1128/AAC.45.12.3474-3481.2001
- Bulai, T., Bratosin, D., Pons, A., Montreuil, J., and Zanetta, J. P. (2003). Diversity of the human erythrocyte membrane sialic acids in relation with blood groups. *FEBS Lett.* 534, 185–189. doi: 10.1016/S0014-5793(02)03838-3
- Bultman, K. M., Kowalski, C. H., and Cramer, R. A. (2017). *Aspergillus fumigatus* virulence through the lens of transcription factors. *Med. Mycol.* 55, 24–38. doi: 10.1093/mmy/myw120
- Carlson, J. E., Tulsieram, L. K., Glaubit, J. C., Luk, V. W., Kauffeldt, C., and Rutledge, R. (1991). Segregation of random amplified DNA markers in F1 progeny of conifers. *Theor. Appl. Genet.* 83, 194–200. doi: 10.1007/BF00226251

- Chotirmall, S. H., Mirkovic, B., Lavelle, G. M., and McElvaney, N. G. (2014). Immuno-evasive *Aspergillus* virulence factors. *Mycopathologia* 178, 363–370. doi: 10.1007/s11046-014-9768-y
- Dixon, D. M., Polak, A., and Walsh, T. J. (1989). Fungus dose-dependent primary pulmonary aspergillosis in immunosuppressed mice. *Infect. Immun.* 57, 1452–1456.
- Erwig, L. P., and Gow, N. A. (2016). Interactions of fungal pathogens with phagocytes. *Nat. Rev. Microbiol.* 14, 163–176. doi: 10.1038/nrmicro.2015.21
- Fischer, E. R., Hansen, B. T., Nair, V., Hoyt, F. H., and Dorward, D. W. (2005). Scanning electron microscopy. *Curr. Protoc. Microbiol.* 25, 2B.2.1–2B.2.47. doi: 10.1002/9780471729259.mc02b02s25
- Fortwendel, J. R., Juvvadi, P. R., Perfect, B. Z., Rogg, L. E., Perfect, J. R., and Steinbach, W. J. (2010). Transcriptional regulation of chitin synthases by calcineurin controls paradoxical growth of *Aspergillus fumigatus* in response to caspofungin. *Antimicrob. Agents Chemother.* 54, 1555–1563. doi: 10.1128/AAC.00854-09
- Fuchs, B. B., and Mylonakis, E. (2009). Our paths might cross: the role of the fungal cell wall integrity pathway in stress response and cross talk with other stress response pathways. *Eukaryot. Cell* 8, 1616–1625. doi: 10.1128/EC.00193-09
- Fuqua, T. H. Jr., Sittitavornwong, S., Knoll, M., and Said-Al-Naief, N. (2010). Primary invasive oral aspergillosis: an updated literature review. *J. Oral Maxillofac. Surg.* 68, 2557–2563. doi: 10.1016/j.joms.2009.08.013
- Ganesan, L. T., Manavathu, E. K., Cutright, J. L., Alangaden, G. J., and Chandrasekar, P. H. (2004). In-vitro activity of nikkomycin Z alone and in combination with polyenes, triazoles or echinocandins against *Aspergillus fumigatus*. *Clin. Microbiol. Infect.* 10, 961–966. doi: 10.1111/j.1469-0691.2004.00996.x
- Gravelat, F. N., Beauvais, A., Liu, H., Lee, M. J., Snarr, B. D., Chen, D., et al. (2013). *Aspergillus* galactosaminogalactan mediates adherence to host constituents and conceals hyphal beta-glucan from the immune system. *PLOS Pathog.* 9:e1003575. doi: 10.1371/journal.ppat.1003575
- Gray, K. C., Palacios, D. S., Dailey, I., Endo, M. M., Uno, B. E., Wilcock, B. C., et al. (2012). Amphotericin primarily kills yeast by simply binding ergosterol. *Proc. Natl. Acad. Sci. U.S.A.* 109, 2234–2239. doi: 10.1073/pnas.1117280109
- Grice, C. M., Bertuzzi, M., and Bignell, E. M. (2013). Receptor-mediated signaling in *Aspergillus fumigatus*. *Front. Microbiol.* 4:26. doi: 10.3389/fmicb.2013.00026
- Hamert, J. E., and Timberlaket, W. E. (1987). Functional organization of the *Aspergillus nidulans trpC* promoter. *Mol. Cell. Biol.* 7, 2352–2359. doi: 10.1128/MCB.7.7.2352
- Hector, R. F. (1993). Compounds active against cell walls of medically important fungi. *Clin. Microbiol. Rev.* 6, 1–21. doi: 10.1128/CMR.6.1.1
- Hill, T. W., and Kafer, E. (2001). Improved protocols for *Aspergillus* minimal medium: trace element and minimal medium salt stock solutions. *Fungal Genet. Newsl.* 48, 20–21. doi: 10.4148/1941-4765.1173
- Inoue, S., and Kitajima, K. (2006). KDN (deaminated neuraminic acid): dreamful past and exciting future of the newest member of the sialic acid family. *Glycoconj. J.* 23, 277–290. doi: 10.1007/s10719-006-6484-y
- Inoue, S., Kitajima, K., and Inoue, Y. (1996). Identification of 2-keto-3-deoxy-D-glycero-galactononic acid (KDN, deaminoneuraminic acid) residues in mammalian tissues and human lung carcinoma cells. chemical evidence of the occurrence of KDN glycoconjugates in animals. *J. Biol. Chem.* 271, 24341–24344. doi: 10.1074/jbc.271.40.24341
- Inoue, S., Lin, S. L., Chang, T., Wu, S. H., Yao, C. W., Chu, T. Y., et al. (1998). Identification of free deaminated sialic acid (2-keto-3-deoxy-D-glycero-D-galacto-nononic acid) in human red blood cells and its elevated expression in fetal cord red blood cells and ovarian cancer cells. *J. Biol. Chem.* 273, 27199–27204. doi: 10.1074/jbc.273.42.27199
- Kanamori, A., Kitajima, K., Inoue, S., and Inoue, Y. (1989). Isolation and characterization of deaminated neuraminic acid-rich glycoprotein (KDN-gp-of) in the ovarian fluid of rainbow trout (*salmo gairdneri*). *Biochem. Biophys. Res. Commun.* 164, 744–749. doi: 10.1016/0006-291X(89)91522-2
- Kim, J. H., Chan, K. L., Faria, N. C., Martins Mde, L., and Campbell, B. C. (2012). Targeting the oxidative stress response system of fungi with redox-potent chemosensitizing agents. *Front. Microbiol.* 3:88. doi: 10.3389/fmicb.2012.00088
- King, S. J., Hippe, K. R., and Weiser, J. N. (2006). Deglycosylation of human glycoconjugates by the sequential activities of exoglycosidases expressed by *Streptococcus pneumoniae*. *Mol. Microbiol.* 59, 961–974. doi: 10.1111/j.1365-2958.2005.04984.x
- Kousha, M., Tadi, R., and Soubani, A. O. (2011). Pulmonary aspergillosis: a clinical review. *Eur. Respir. Rev.* 20, 156–174. doi: 10.1183/09059180.00001011
- Lass-Florl, C., and Cuenca-Estrella, M. (2017). Changes in the epidemiological landscape of invasive mould infections and disease. *J. Antimicrob. Chemother.* 72(Suppl. 1), i5–i11. doi: 10.1093/jac/dkx028
- Lee, M. J., and Sheppard, D. C. (2016). Recent advances in the understanding of the *Aspergillus fumigatus* cell wall. *J. Microbiol.* 54, 232–242. doi: 10.1007/s12275-016-6045-4
- Malavazi, I., da Silva, Ferreira, M. E., Soriani, F. M., Dinamarco, T. M., Savoldi, M., et al. (2009). Phenotypic analysis of genes whose mRNA accumulation is dependent on calcineurin in *Aspergillus fumigatus*. *Fungal Genet. Biol.* 46, 791–802. doi: 10.1016/j.fgb.2009.06.009
- Maus, U. A., Waelsch, K., Kuziel, W. A., Delbeck, T., Mack, M., Blackwell, T. S., et al. (2003). Monocytes are potent facilitators of alveolar neutrophil emigration during lung inflammation: role of the CCL2-CCR2 axis. *J. Immunol.* 170, 3273–3278. doi: 10.4049/jimmunol.170.6.3273
- May, M., Szczepanek, S. M., Frasca, S. Jr., Gates, A. E., Demcovitz, D. L., Moneypenny, C. G., et al. (2012). Effects of sialidase knockout and complementation on virulence of *Mycoplasma gallisepticum*. *Vet. Microbiol.* 157, 91–95. doi: 10.1016/j.vetmic.2011.12.004
- McCormick, A., Jacobsen, I. D., Broniszewska, M., Beck, J., Heesemann, J., and Ebel, F. (2012). The two-component sensor kinase tscC and its role in stress resistance of the human-pathogenic mold *Aspergillus fumigatus*. *PLOS ONE* 7:e38262. doi: 10.1371/journal.pone.0038262
- Mesa-Arango, A. C., Scorzoni, L., and Zaragoza, O. (2012). It only takes one to do many jobs: amphotericin B as antifungal and immunomodulatory drug. *Front. Microbiol.* 3:286. doi: 10.3389/fmicb.2012.00286
- Mignone, F., Gissi, C., Liuni, S., and Pesole, G. (2002). Untranslated regions of mRNAs. *Genome Biol.* 3, reviews0004.1–reviews0004.10 doi: 10.1186/gb-2002-3-3-reviews0004
- Muszkieta, L., Aimanian, V., Mellado, E., Gribaldo, S., Alcazar-Fuoli, L., Szcwzyk, E., et al. (2014). Deciphering the role of the chitin synthase families 1 and 2 in the *in vivo* and *in vitro* growth of *Aspergillus fumigatus* by multiple gene targeting deletion. *Cell. Microbiol.* 16, 1784–1805. doi: 10.1111/cmi.12326
- Nadano, D., Iwasaki, M., Endo, S., Kitajima, K., Inoue, S., and Inoue, Y. (1986). A naturally occurring deaminated neuraminic acid, 3-deoxy-D-glycero-D-galacto-nonulosonic acid (KDN): its unique occurrence at the nonreducing ends of oligosialyl chains in polysialoglycoprotein of rainbow trout eggs. *J. Biol. Chem.* 261, 11550–11557.
- Nishino, S., Kuroyanagi, H., Terada, T., Inoue, S., Inoue, Y., Troy, F. A., et al. (1996). Induction, localization, and purification of a novel sialidase, deaminoneuraminidase (KDNase), from *Sphingobacterium multivorum*. *J. Biol. Chem.* 271, 2909–2913. doi: 10.1074/jbc.271.6.2909
- Nivoix, Y., Velten, M., Letscher-Bru, V., Moghaddam, A., Natarajan-Ame, S., Fohrer, C., et al. (2008). Factors associated with overall and attributable mortality in invasive aspergillosis. *Clin. Infect. Dis.* 47, 1176–1184. doi: 10.1086/592255
- Odds, F. C., Brown, A. J., and Gow, N. A. (2003). Antifungal agents: mechanisms of action. *Trends Microbiol.* 11, 272–279. doi: 10.1016/S0966-842X(03)00117-3
- Ostash, B., Shashkov, A., Streshinskaya, G., Tul'skaya, E., Baryshnikova, L., Dmitrenok, A., et al. (2014). Identification of *Streptomyces coelicolor* M145 genomic region involved in biosynthesis of teichulosonic acid-cell wall glycopolymer. *Folia Microbiol.* 59, 355–360. doi: 10.1007/s12223-014-0306-6
- Palacios, D. S., Dailey, I., Siebert, D. M., Wilcock, B. C., and Burke, M. D. (2011). Synthesis-enabled functional group deletions reveal key underpinnings of amphotericin B ion channel and antifungal activities. *Proc. Natl. Acad. Sci. U.S.A.* 108, 6733–6738. doi: 10.1073/pnas.1015023108
- Palese, P., Tobita, K., Ueda, M., and Compans, R. W. (1974). Characterization of temperature sensitive influenza virus mutants defective in neuraminidase. *Virology* 61, 397–410. doi: 10.1016/0042-6822(74)90276-1
- Philippe, B., Ibrahim-Granet, O., Prevost, M. C., Gougerot-Pocidalo, M. A., Sanchez Perez, M., Van der Meer, A., et al. (2003). Killing of *Aspergillus fumigatus* by alveolar macrophages is mediated by reactive oxidant intermediates. *Infect. Immun.* 71, 3034–3042. doi: 10.1128/IAI.71.6.3034-3042.2003

- Robinet, P., Baychelier, F., Fontaine, T., Picard, C., Debre, P., Vieillard, V., et al. (2014). A polysaccharide virulence factor of a human fungal pathogen induces neutrophil apoptosis via NK cells. *J. Immunol.* 192, 5332–5342. doi: 10.4049/jimmunol.1303180
- Rocha, M. C., de Godoy, K. F., de Castro, P. A., Hori, J. I., Pedro Bom, V. L., Brown, N. A., et al. (2015). The *Aspergillus fumigatus* *pkcA*^{G579R} mutant is defective in the activation of the cell wall integrity pathway but is dispensable for virulence in a neutropenic mouse infection model. *PLoS ONE* 10:e0135195. doi: 10.1371/journal.pone.0135195
- Roncero, C., and Duran, A. (1985). Effect of calcofluor white and congo red on fungal cell wall morphogenesis: in vivo activation of chitin polymerization. *J. Bacteriol.* 163, 1180–1185.
- Sánchez, O., and Aguirre, J. (1996). Efficient transformation of *Aspergillus nidulans* by electroporation of germinated conidia. *Fungal Genet. Newsl.* 43, 48–51. doi: 10.4148/1941-4765.1317
- Sangalli-Leite, F., Scorzoni, L., Mesa-Arango, A. C., Casas, C., Herrero, E., Gianinni, M. J., et al. (2011). Amphotericin B mediates killing in *Cryptococcus neoformans* through the induction of a strong oxidative burst. *Microbes Infect.* 457–467. doi: 10.1016/j.micinf.2011.01.015
- Schaffner, A., Douglas, H., and Braude, A. (1982). Selective protection against conidia by mononuclear and against mycelia by polymorphonuclear phagocytes in resistance to *Aspergillus*. Observations on these two lines of defense in vivo and in vitro with human and mouse phagocytes. *J. Clin. Invest.* 69, 617–631. doi: 10.1172/JCI110489
- Scharf, D. H., Heinekamp, T., and Brakhage, A. A. (2014). Human and plant fungal pathogens: the role of secondary metabolites. *PLoS Pathog.* 10:e1003859. doi: 10.1371/journal.ppat.1003859
- Schmiedel, Y., and Zimmerli, S. (2016). Common invasive fungal diseases: an overview of invasive candidiasis, aspergillosis, cryptococcosis, and pneumocystis pneumonia. *Swiss Med. Wkly.* 146:w14281. doi: 10.4414/smw.2016.14281
- Shashkov, A. S., Tul'skaya, E. M., Evtushenko, L. I., Denisenko, V. A., Ivanyuk, V. G., Stomakhin, A. A., et al. (2002). Cell wall anionic polymers of *Streptomyces* Sp. MB-8, the causative agent of potato scab. *Carbohydr. Res.* 337, 2255–2261. doi: 10.1016/S0008-6215(02)00188-X
- Silar, P. (1995). Two new easy to use vectors for transformations. *Fungal Genet. Newsl.* 42, 73. doi: 10.4148/1941-4765.1353
- Smutova, V., Albohy, A., Pan, X., Korchagina, E., Miyagi, T., Bovin, N., et al. (2014). Structural basis for substrate specificity of mammalian neuraminidases. *PLoS ONE* 9:e106320. doi: 10.1371/journal.pone.0106320
- Song, Y., Kitajima, K., Inoue, S., and Inoue, Y. (1991). Isolation and structural elucidation of a novel type of ganglioside, deaminated neuraminic acid (KDN)-containing glycosphingolipid, from rainbow trout sperm. The first example of the natural occurrence of kdn-ganglioside, (KDN)GM3. *J. Biol. Chem.* 266, 21929–21935.
- Strecker, G., Wieruszkeski, J. M., Michalski, J. C., Alonso, C., Boilly, B., and Montreuil, J. (1992). Characterization of Le^x, Le^y and A Le^y antigen determinants in kdn-containing o-linked glycan chains from *Pleurodeles waltl*ii jelly coat eggs. *FEBS Lett.* 298, 39–43. doi: 10.1016/0014-5793(92)80018-C
- Sturtevant, J., and Latge, J. P. (1992). Participation of complement in the phagocytosis of the conidia of *Aspergillus fumigatus* by human polymorphonuclear cells. *J. Infect. Dis.* 166, 580–586. doi: 10.1093/infdis/166.3.580
- Telford, J. C., Yeung, J. H., Xu, G., Kiefel, M. J., Watts, A. G., Hader, S., et al. (2011). The *Aspergillus fumigatus* sialidase is a 3-deoxy-D-glycero-D-galactose-2-nuloseonic acid hydrolase (KDNase): structural and mechanistic insights. *J. Biol. Chem.* 286, 10783–10792. doi: 10.1074/jbc.M110.207043
- Urbina, J. A., Cohen, B. E., Perozo, E., and Cornivelli, L. (1987). Spin-labeled amphotericin B: synthesis, characterization, biological and spectroscopic properties. *Biochim. Biophys. Acta* 897, 467–473. doi: 10.1016/0005-2736(87)90443-3
- Valiante, V., Macheleidt, J., Foge, M., and Brakhage, A. A. (2015). The *Aspergillus fumigatus* cell wall integrity signaling pathway: drug target, compensatory pathways, and virulence. *Front. Microbiol.* 6:325. doi: 10.3389/fmicb.2015.00325
- Varki, A., and Schauer, R. (2009). "Sialic acids," in *Essentials of Glycobiology*, 2nd Edn, eds A. Varki, R. D. Cummings, J. D. Esko, H. H. Freeze, P. Stanley, C. R. Bertozzi et al. (Cold Spring Harbor, NY: Cold Spring Harbor Laboratory Press).
- von Itzstein, M. (2007). The war against influenza: discovery and development of sialidase inhibitors. *Nat. Rev. Drug Discov.* 6, 967–974. doi: 10.1038/nrd2400
- Walsh, T. J., Anaissie, E. J., Denning, D. W., Herbrecht, R., Kontoyannis, D. P., Marr, K. A., et al. (2008). Treatment of aspergillosis: clinical practice guidelines of the infectious diseases society of America. *Clin. Infect. Dis.* 46, 327–360. doi: 10.1086/525258
- Warwas, M. L., Watson, J. N., Bennet, A. J., and Moore, M. M. (2007). Structure and role of sialic acids on the surface of *Aspergillus fumigatus* conidiospores. *Glycobiology* 17, 401–410. doi: 10.1093/glycob/cwl085
- Warwas, M. L., Yeung, J. H., Indrugalla, D., Mooers, A. O., Bennet, A. J., and Moore, M. M. (2010). Cloning and characterization of a sialidase from the filamentous fungus, *Aspergillus fumigatus*. *Glycoconj. J.* 27, 533–548. doi: 10.1007/s10719-010-9299-9
- Wasylnka, J. A., and Moore, M. M. (2000). Adhesion of *Aspergillus* species to extracellular matrix proteins: evidence for involvement of negatively charged carbohydrates on the conidial surface. *Infect. Immun.* 68, 3377–3384. doi: 10.1128/IAI.68.6.3377-3384.2000
- Wasylnka, J. A., and Moore, M. M. (2002). Uptake of *Aspergillus fumigatus* conidia by phagocytic and nonphagocytic cells in vitro: quantitation using strains expressing green fluorescent protein. *Infect. Immun.* 70, 3156–3163. doi: 10.1128/IAI.70.6.3156-3163.2002
- Wasylnka, J. A., and Moore, M. M. (2003). *Aspergillus fumigatus* conidia survive and germinate in acidic organelles of a549 epithelial cells. *J. Cell Sci.* 116, 1579–1587. doi: 10.1242/jcs.00329
- Wasylnka, J. A., Simmer, M. I., and Moore, M. M. (2001). Differences in sialic acid density in pathogenic and non-pathogenic *Aspergillus* species. *Microbiology* 147, 869–877. doi: 10.1099/00221287-147-4-869
- Wiedemann, A., Spadinger, A., Löwe, A., Seeger, A., and Ebel, F. (2016). Agents that activate the high osmolarity glycerol pathway as a means to combat pathogenic molds. *Int. J. Med. Microbiol.* 306, 642–651. doi: 10.1016/j.ijmm.2016.09.005
- Wiederhold, N. P. (2007). Attenuation of echinocandin activity at elevated concentrations: a review of the paradoxical effect. *Curr. Opin. Infect. Dis.* 20, 574–578. doi: 10.1097/QCO.0b013e3282f1be7f
- Yamaguchi, H., Uchida, K., Nagino, K., and Matsunaga, T. (2002). Usefulness of a colorimetric method for testing antifungal drug susceptibilities of *Aspergillus* species to voriconazole. *J. Infect. Chemother.* 8, 374–377. doi: 10.1007/s10156-002-0201-y
- Young, R. C., Bennett, J. E., Vogel, C. L., Carbone, P. P., and DeVita, V. T. (1970). Aspergillosis. The spectrum of the disease in 98 Patients. *Medicine* 49, 147–173. doi: 10.1097/00005792-197003000-00002
- Zhang, Y., and Sachs, M. S. (2015). Control of mRNA stability in fungi by NMD, EJC and CBC factors through 3'UTR introns. *Genetics* 200, 1133–1148. doi: 10.1534/genetics.115.176743

Conflict of Interest Statement: The authors declare that the research was conducted in the absence of any commercial or financial relationships that could be construed as a potential conflict of interest.

Copyright © 2018 Nesbitt, Steves, Schonhofer, Cait, Manku, Yeung, Bennet, McNagny, Choy, Hughes and Moore. This is an open-access article distributed under the terms of the Creative Commons Attribution License (CC BY). The use, distribution or reproduction in other forums is permitted, provided the original author(s) or licensor are credited and that the original publication in this journal is cited, in accordance with accepted academic practice. No use, distribution or reproduction is permitted which does not comply with these terms.